Geoscience Frontiers 9 (2018) 1921–1936

HOSTED BY

ELSEVIER

Contents lists available at ScienceDirect

China University of Geosciences (Beijing)

Geoscience Frontiers

journal homepage: www.elsevier.com/locate/gsf

Research Paper

Cold plumes trigger contamination of oceanic mantle wedges with continental crust-derived sediments: Evidence from chromitite zircon grains of eastern Cuban ophiolites

J.A. Proenza [a,*], J.M. González-Jiménez [b], A. Garcia-Casco [b,c], E. Belousova [d], W.L. Griffin [d], C. Talavera [e], Y. Rojas-Agramonte [f,g], T. Aiglsperger [a], D. Navarro-Ciurana [a], N. Pujol-Solà [a], F. Gervilla [b,c], S.Y. O'Reilly [d], D.E. Jacob [d]

[a] Departament de Mineralogia, Petrologia i Geologia Aplicada, Universitat de Barcelona, C/Martí i Franquès s/n, 08028, Barcelona, Spain
[b] Departamento de Mineralogía y Petrología, Universidad de Granada, Facultad de Ciencias, Fuentenueva s/n 18002, Granada, Spain
[c] Instituto Andaluz de Ciencias de la Tierra (CSIC-UGR), Avda. de las Palmeras 4, E-18100, Armilla, Granada, Spain
[d] ARC Centre of Excellence for Core to Crust Fluid Systems (CCFS), GEMOC National Key Centre, Department of Earth and Planetary Sciences, Macquarie University, Sydney, NSW 2109, Australia
[e] John de Laeter Centre, Curtin University, Perth, WA 6102, Australia
[f] Geocycles-Earth System Research Center, Institut für Geowissenschaften, Johannes Gutenberg-Universität, Becherweg 21, D-55099 Mainz, Germany
[g] Departamento de Geociencias, Universidad de los Andes, Bogotá, Colombia

ARTICLE INFO

Article history:
Received 15 September 2017
Received in revised form
23 November 2017
Accepted 10 December 2017
Available online 30 December 2017
Handling Editor: M. Santosh

Keywords:
Zircon
U-Pb geochronology
Chromitites
Cold plumes
Ophiolites
Cuba

ABSTRACT

The origin of zircon grains, and other exotic minerals of typical crustal origin, in mantle-hosted ophiolitic chromitites are hotly debated. We report a population of zircon grains with ages ranging from Cretaceous (99 Ma) to Neoarchean (2750 Ma), separated from massive chromitite bodies hosted in the mantle section of the supra-subduction (SSZ)-type Mayarí-Baracoa Ophiolitic Belt in eastern Cuba. Most analyzed zircon grains ($n = 20$, 287 ± 3 Ma to 2750 ± 60 Ma) are older than the early Cretaceous age of the ophiolite body, show negative $\varepsilon_{Hf}(t)$ (-26 to -0.6) and occasional inclusions of quartz, K-feldspar, biotite, and apatite that indicate derivation from a granitic continental crust. In contrast, 5 mainly rounded zircon grains (297 ± 5 Ma to 2126 ± 27 Ma) show positive $\varepsilon_{Hf}(t)$ ($+0.7$ to $+13.5$) and occasional apatite inclusions, suggesting their possible crystallization from melts derived from juvenile (mantle) sources. Interestingly, younger zircon grains are mainly euhedral to subhedral crystals, whereas older zircon grains are predominantly rounded grains. A comparison of the ages and Hf isotopic compositions of the zircon grains with those of nearby exposed crustal terranes suggest that chromitite zircon grains are similar to those reported from terranes of Mexico and northern South America. Hence, chromitite zircon grains are interpreted as sedimentary-derived xenocrystic grains that were delivered into the mantle wedge beneath the Greater Antilles intra-oceanic volcanic arc by metasomatic fluids/melts during subduction processes. Thus, continental crust recycling by subduction could explain all populations of old xenocrystic zircon in Cretaceous mantle-hosted chromitites from eastern Cuba ophiolite. We integrate the results of this study with petrological-thermomechanical modeling and existing geodynamic models to propose that ancient zircon xenocrysts, with a wide spectrum of ages and Hf isotopic compositions, can be transferred to the mantle wedge above subducting slabs by cold plumes.

1. Introduction

Recent reports of inherited (i.e. xenocrystic) zircon grains found in supra-subduction zone ophiolitic and juvenile intra-oceanic volcanic arc rocks, with ages and isotopic signatures similar to zircon grains typically found in granites of the continental crust, have been

* Corresponding author.
E-mail address: japroenza@ub.edu (J.A. Proenza).
Peer-review under responsibility of China University of Geosciences (Beijing).

https://doi.org/10.1016/j.gsf.2017.12.005

interpreted as evidence of the recycling of supracrustal material within the subduction factory (e.g., Rojas-Agramonte et al., 2016 and references therein). Similarly, old xenocrystic zircon grains bearing both, crustal and juvenile geochemical signatures, are being increasingly found in chromitite bodies hosted in the upper mantle sections of ophiolitic complexes (Robinson et al., 2004, 2015; Lönngren and Kojonen, 2005; Savelieva et al., 2006, 2007; Yamamoto et al., 2013; Belousova et al., 2015; González-Jiménez et al., 2015; Akbulut et al., 2016; Griffin et al., 2016; Lian et al., 2017; González-Jiménez et al., 2017a), and are also interpreted as mineralogical evidence for the passage of crustal material through the mantle, prior to its return to the shallow lithospheric mantle. The latter interpretation is supported by the fact that many chromitite zircon grains are mostly rounded suggesting sedimentary transport, resorption and overgrowths (e.g., Robinson et al., 2015). Furthermore, these xenocrystic zircon grains in chromitites hosted in the oceanic mantle are usually accompanied by other exotic minerals of typical continental crustal origin (e.g., quartz, K-feldspar, corundum, kyanite, andalusite, almandine garnet, apatite, rutile, titanite) (Yang et al., 2015; Robinson et al., 2015 and references therein).

The mechanisms for recycling of crustal material into the mantle are varied and include both subduction or delamination and detachment of continental crust (e.g., Bea et al., 2001; Stern, 2002; Gao et al., 2004; Scholl and von Huene, 2009; Spandler and Pirard, 2013; Yamamoto et al., 2013; Zhou et al., 2014; Robinson et al., 2015; Rojas-Agramonte et al., 2016), which can be temporally and spatially related to the chromitite-forming event. Furthermore, the occurrence of diamond, moissanite and other ultra-high pressure (UHP) and ultrareduced phases in the same chromitite bodies suggests recycling into the deep mantle down to the transition zone (TZ) and, perhaps, deeper (e.g., Arai, 2013; McGowan et al., 2015; Yang et al., 2015; Griffin et al., 2016). Ascent of TZ material to shallow lithospheric depths has been related to mantle plume which rose through the TZ (Yang et al., 2014, 2015; Xiong et al., 2015; Xu et al., 2015) or with slab roll-back (McGowan et al., 2015; Griffin et al., 2016).

On the other hand, Belousova et al. (2015) have provided an alternative hypothesis to explain the formation of ancient crustal zircon grains in chromitites from the Coolac serpentinite belt (New South Wales, Australia). In this case, the crustally derived zircon grains were physically introduced into the ophiolitic mantle chromitites after their obduction by melts/fluids derived from neighboring granite intrusions via a microscopic melt network. In addition, some zircon grains, with euhedral morphology and magmatic zoning in mantle-hosted ophiolitic chromitite, have been related to the timing of chromitite formation. The Hf and O isotope composition of these zircon grains suggest mixing between mantle-derived and slab (crustal component)-derived melts (McGowan et al., 2015; Griffin et al., 2016).

This new question in geoscience can be solved in scenarios where the populations of zircon grains in both the mantle and the corresponding overlying crust have similar ages and geochemical signatures. Suprasubduction zone (SSZ) ophiolites are the best candidates, as in these tectonic setting the mantle wedge above the subduction zone and the oceanic or arc crust is generally preserved. The island of Cuba hosts one of the largest SSZ ophiolite belts in the world, and in its easternmost part (the so-called Mayarí-Baracoa Ophiolitic Belt: MBOB; Fig. 1a) a portion of strongly depleted upper mantle, which was criptically metasomatized by slab-derived fluids with sedimentary contributions, is associated with a complementary oceanic arc crust (Proenza et al., 1999; Marchesi et al., 2006, 2007). The recent discovery of crustal zircon grains in the Cretaceous gabbros of the MBOB (Rojas-Agramonte et al., 2016), complementary to a mantle section containing chromitite bodies, offers an unique scenario for evaluating the recycling of crustal material in the mantle and tracking return pathways to the Earth's surface.

In the present study we used the most innovative techniques of mineral separation (Selfrag) and concentration (Hydroseparation) for obtain heavy minerals (including zircon grains) from several chromite deposits of the MBOB. These deposits include the different compositional chromite types known in ophiolites (i.e., high-Cr and high-Al composition) and represent different levels of the mantle section (from relatively deep mantle to the uppermost part of the mantle-crust transition). We present *in situ* SHRIMP and LA-(MC)-ICPMS U-Pb dating and Hf isotope compositions of the recovered zircon grains in order to constrain the age and character of the fluids/melts from which they crystallized. The presence of old xenocrystic zircon grains with both crustal and juvenile signatures within the chromitites of the MBOB is integrated with recent regional geochemical and petrological data and paleotectonic models of the region to offer an explanation for the presence of old zircon grains in the Cretaceous Caribbean oceanic mantle.

2. Geological setting

The geology of eastern Cuba is dominated by oceanic units of Early to Late Cretaceous volcanic arc sequences, the Mayarí-Baracoa ophiolitic belt, and associated Early Cretaceous high-pressure serpentinite-matrix subduction mélanges (Sierra del Convento and La Corea) and a Late Cretaceous metamorphic sole (the Güira de Jauco Amphibolite Complex) (Iturralde-Vinent, 1996; Proenza et al., 1999, 2006; Iturralde-Vinent et al., 2006; Garcia-Casco et al., 2006, 2008a, b; Lázaro et al., 2009, 2015; Blanco-Quintero et al., 2011a, b, c; Fig. 1b). These units constitute tectonic nappes with a general vergence of thrusting towards the NE and accreted in the Late Cretaceous–Earliest Palaeocene (e.g., Iturralde-Vinent, 1996; Cobiella-Reguera, 2005; Iturralde-Vinent et al., 2006). Other lithotectonic associations in eastern Cuba are the Late Cretaceous HP metasedimentary rocks of the Asunción terrane, and Maastrichtian–Danian synorogenic deposits of La Picota and Mícara formations (Iturralde-Vinent, 1996, Iturralde-Vinent et al., 2006; Garcia-Casco et al., 2008a; Fig. 1b).

2.1. Cuban ophiolites: the Mayarí-Baracoa ophiolitic belt (MBOB)

The Mesozoic ophiolitic bodies of Cuba (the so-called Northern Cuban Ophiolite Belt, NCOB, in west-central Cuba; and the Mayarí-Baracoa Ophiolite Belt, MBOB, located in eastern Cuba) form a discontinuous belt more than 1000 km in length that constitutes the most extensive surface exposure of oceanic lithosphere in the circum-Caribbean region (Fig. 1a; Iturralde-Vinent, 1996; Cobiella-Reguera, 2005; Garcia-Casco et al., 2006; Lewis et al., 2006; Iturralde-Vinent et al., 2016). These ophiolites represent slices of oceanic lithosphere obducted onto the North American continental paleo-margin in Latest Cretaceous to Late Eocene time during the collision between the leading edge of the Caribbean plate (volcanic arc of the Caribbean) with Jurassic–Cretaceous passive margins of the continental Maya block and the Bahamas platform (Iturralde-Vinent, 1996; Garcia-Casco et al., 2008a, b).

The ophiolite assemblage of the MBOB (170 km long, 10–30 km wide, average 3.5 km thick; Fig. 1a; Iturralde-Vinent, 1996; Proenza et al., 1999; Marchesi et al., 2006) is highly dismembered and constitutes a portion of MOR-like lithosphere modified in a suprasubduction zone related to the intra-oceanic Greater Antilles arc, developed during the Lower-Upper Cretaceous (Proenza et al., 1999). The MBOB hosts sections of mantle tectonite harzburgite, Moho transition zone (MTZ), layered gabbros and mafic volcanic rocks (Proenza et al., 1999; Lewis et al., 2006; Marchesi et al., 2006; Iturralde-Vinent et al., 2016). Major fault zones separate the MBOB into two individual thrust-bounded blocks ("massif"), namely the

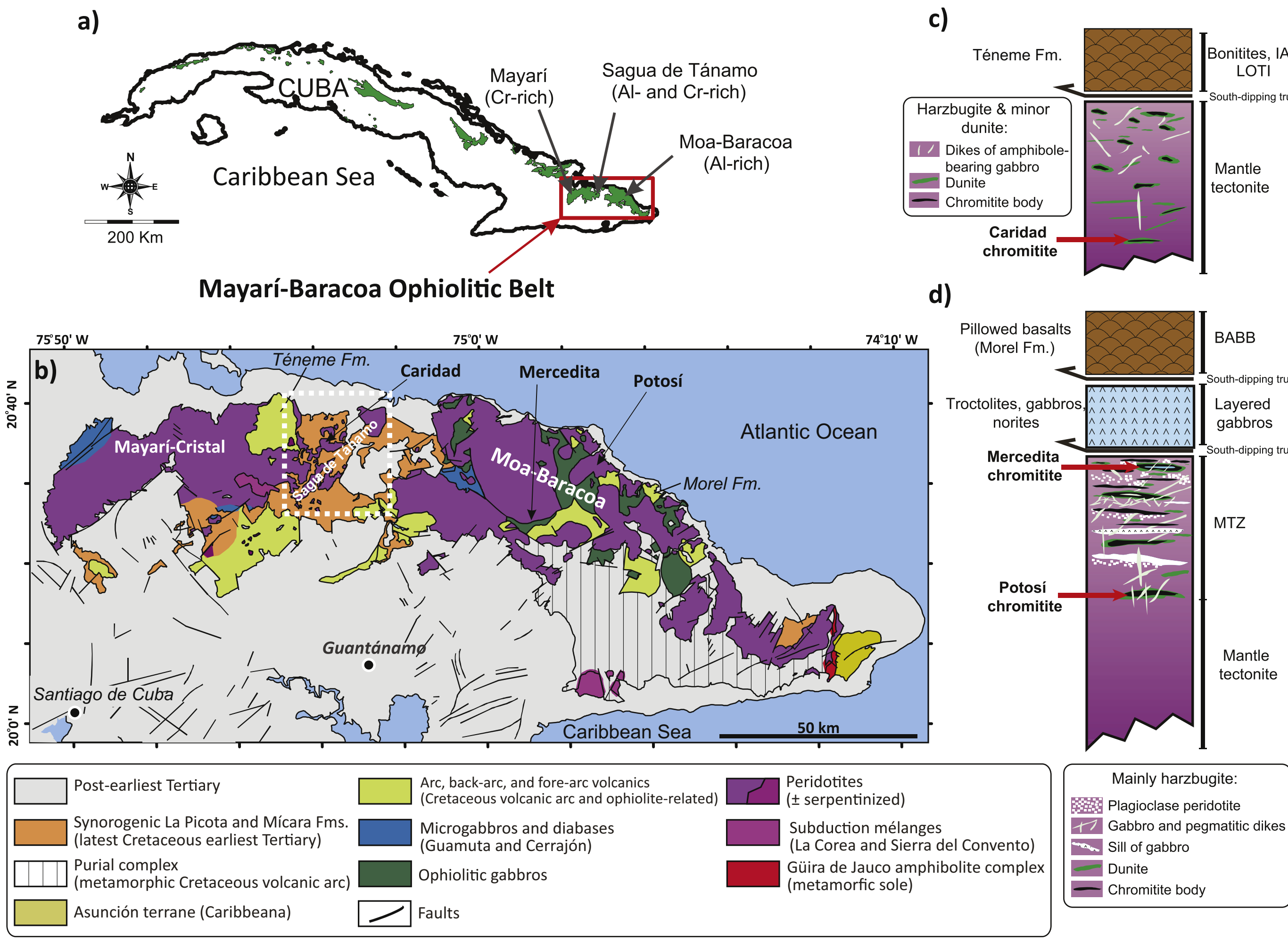

Figure 1. (a) Geographic location of massifs constituting the Northern Cuban Ophiolite Belt; red box indicates the Mayarí-Baracoa Ophiolitic Belt (MBOB) in eastern Cuba. (b) Geological map of the MBOB (Pushcharovsky, 1988) with location of studied chromitite samples. Schematic lithostratigraphic columns of Sagua de Tánamo (c) and Moa-Baracoa (d) areas with location of studied chromitites.

Mayarí-Cristal massif to the west and the Moa-Baracoa massif to the east (Fig. 1b).

2.1.1. The Mayarí-Cristal massif

The Mayarí-Cristal massif is made up mainly of highly serpentinized harzburgite tectonite (>5 km thick) hosting subconcordant and discordant dunite bodies that often enclose chromitite bodies (Fig. 1b and c). The peridotites are locally cut by several generations of websterite and gabbroic dykes of IAT affinity (Marchesi et al., 2006). The easternmost part of the massif (Sagua de Tánamo region; Fig. 1) is composed of highly serpentinized mantle tectonites (dunite and harzburgite), which are tectonically emplaced onto the Turonian to Early Coniacioan forearc-related volcanic rocks of the Teìneme Formation and the Maastrichtian–Danian olistostromic synorogenic rocks of Micara and La Picota formations (Fig. 1b) (Proenza et al., 2006; Iturralde-Vinent et al., 2006; Marchesi et al., 2006, 2007). Basaltic rocks of the Teìneme Fm. are low-Ti island-arc tholeiites with boninitic affinity, and have been interpreted as formed in a fore-arc environment during the early stages of subduction (Proenza et al., 2006).

2.1.2. The Moa-Baracoa massif

The Moa-Baracoa is made up of a ~2.2 km thick section of mantle-tectonite harzburgite with subordinate dunite and a MTZ crosscut by gabbroic dikes (locally pegmatitic) associated with layered and isotropic gabbro sequence (~500 m thick; Fig. 1b, d). Peridotites and layered and isotropic gabbros of the Moa-Baracoa massif are in tectonic contact with pillow basalts of the Turonian-Coniacian Morel Formation (88–91 Ma; Iturralde-Vinent et al., 2006) with a back-arc geochemical affinity (Proenza et al., 2006; Marchesi et al., 2007). Marchesi et al. (2006) showed that cumulate gabbros from this massif and Morel back-arc volcanics show similar geochemical affinities and proposed a genetic link. In general, a forearc setting is suggested for the formation of the Mayarí-Cristal Ophiolite Massif, whereas the Moa-Baracoa Ophiolite Massif was formed in a backarc environment (Gervilla et al., 2005; Proenza et al., 2006; Blanco-Quintero et al., 2011b; Lázaro et al., 2015).

2.2. The chromite deposits

More than 250 chromite deposits and occurrences have been described in the MBOB (Proenza et al., 1999, 2001a; Gervilla et al., 2005; González-Jiménez et al., 2011). Proenza et al. (1999) grouped these chromitite bodies into three mining districts according to the composition of chromite, from west to east: Mayarí, Sagua de Tánamo and Moa-Baracoa (Fig. 1).

The Mayarí district is located in the western part of the Mayarí-Cristal massif and includes small to medium-sized high-Cr chromitite bodies (Cr# = Cr/[Cr + Al] = 0.70–0.83; $TiO_2 < 0.2$ wt.%; Proenza et al., 1999; Gervilla et al., 2005). These are pod-shaped and are located deep in the mantle section of the massif, and exhibit dunite envelopes of variable thickness. They are concordant to the high-temperature foliation of the enclosing peridotite. Dykes and veins of pyroxenites (mainly websterites) often crosscut these chromitite bodies.

Both high-Cr and high-Al chromitite varieties (Cr# = 0.45–0.74; TiO_2 = 0.1–0.3 wt.%) occur interspersed within the small district of Sagua de Tánamo in the easternmost part of the Mayarí-Cristal Massif (Proenza et al., 1999; Gervilla et al., 2005; González-Jiménez et al., 2011). Chromitite bodies are small and variable in size (30–40 m long, 10–20 m wide, 1–3 m thick) and have tabular to lenticular shapes. These chromitites are also enclosed in serpentinized dunite pods widespread within the upper-mantle harzburgite and are both concordant and discordant to the foliation of the host peridotite (Fig. 1c). However, some chromitite bodies host concordant lenses and cross-cutting dykes of fine to coarse-grained amphibole-bearing gabbro.

The Moa-Baracoa district comprises the whole Moa-Baracoa massif and contains bodies of high-Al chromitite (Cr# = 0.41–0.54) and variable TiO_2 (0.05–0.52 wt.%). These chromitites have tabular to lenticular shapes, show variably thick dunite envelopes, and are concordant to the foliation of the host peridotite. Proenza et al. (1999, 2001a) showed that chromitite invaded and replaced a first generation of gabbro sills in dunite, whereas a second generation of gabbroic dykes crosscut them (Fig. 1d).

Calculated melts in equilibrium with the Al-rich chromitites are close to the composition of back-arc basin basalts (BABB), whereas the melts in equilibrium with the Cr-rich chromitites are of magnesian andesitic or boninitic affinity (Proenza et al., 1999; Gervilla et al., 2005; González-Jiménez et al., 2011). This coexistence of high-Cr and high-Al chromitites related to contrasted magmatic liquids reflects the spatial distribution of intrusions of arc-related mantle-derived magmas (boninites, IAT and BABB) in a long-lasting mantle wedge of the northern Caribbean suprasubduction zone.

3. Sampling and analytical methods

3.1. Chromitite samples

Zircon grains analyzed in this study were separated from three different chromite deposits, namely the high-Cr chromite deposit of Caridad hosted in the deeper upper- mantle tectonite of the Sagua de Tánamo district in the easternmost part of Mayarí-Cristal massif; and from the high-Al chromite deposits of Mercedita and Potosí located in the MTZ exposed in the Moa-Baracoa massif (Fig. 1; Proenza et al., 1999; González-Jiménez et al., 2011).

The chromite deposit of Caridad is a small body (up to 5 m thick and up to 10 m long) that occurs within a dunite lens lying concordantly in the tectonite mantle harzburgite (Figs. 1b, c and 2a). Massive-textured ore is the most common type, but disseminated and banded-textured ore occurs towards the external parts of the body (Proenza et al., 1999; Gervilla et al., 2005; González-Jiménez et al., 2011). Zircon grains were extracted from massive chromitite bands (Caridad sample; Fig. 2a) which are almost entirely composed of unaltered Cr-rich chromite (Cr# = 0.7) and minor olivine grains partially replaced by serpentine and minor clinochlore.

The Mercedita deposit is located in the southernmost part of the Moa-Baracoa massif (Fig. 1b) and is the largest ophiolitic chromite deposit in the Americas. The largest body has a lateral extension of 600 m, a width of 250 m, and a thickness of up to 20 m (Proenza et al., 1998, 1999). The chromitite is enclosed in a dunite envelope of variable width (some centimeters to several meters), which is hosted in harzburgite of the MTZ around 250 m below the layered gabbro unit (Figs. 1d and 2b). The chromite ore is concordant with the main structure of the enclosing peridotite and often enclose gabbro bodies (sills). The zircon-bearing sample studied here is a massive chromitite (Mercedita sample; Fig. 2b) made up by 95% of unaltered high-Al chromite (Cr# = 0.47) with accessory olivine, and secondary serpentine and clinochlore.

The Potosí chromite deposit is located in the Moa-Baracoa massif (Fig. 1b) and occurs in dunite bodies within the MTZ, around 800 m below the layered gabbro unit (Fig. 1d; Proenza et al., 2001a). The ore deposit has a lateral extension about 220 m and 8 to 25 m wide. Chromitites are found in lenses with extremely variable size and irregular shapes, from tabular to lenticular. Proenza et al. (2001a) showed that these chromite bodies are intruded by pegmatitic gabbroic dikes (Fig. 2c), representing a late episode of intrusion of basaltic magma. The intrusion of the pegmatitic gabbro followed the direction of pull-apart fractures in the chromitites, which give rise to brecciated chromite ores made up of massive chromitite blocks embedded in a matrix of olivine-rich norite (Proenza et al., 2001a, b). Zircon grains were extracted from this type of chromite ore (Potosí sample, a breccia-textured chromitite with Cr# = 0.5; Fig. 2c).

3.2. Zircon separation and concentration

Zircon grains were recovered from massive chromitite samples using two different methods. A set of 5 zircon grains was recovered from the Caridad chromitite using the high-voltage electric pulsed SelFrag rock disaggregation facility at the Geochemical Analysis Unit, CCFS (GEMOC, Australia). A total of 2 kg of chromitite was split into samples of 200–300 g in successive cycles and the whole system was cleaned with water between each cycle to avoid any possible contamination. The split sample was sieved to a fraction < 210 μm and the sieved material was spread in metallic trays and oven-dried at 80 °C. The dried material was processed by several cycles of magnetic separation with increasing magnetic field using a Frantz electro-magnetic separator. Finally, zircon grains were hand-picked under a Leica UV microscope, mounted in 25 mm epoxy resin discs and polished.

Another set of 21 zircon grains was obtained after processing 2.7 and 0.5 kg of chromitite from the Mercedita (4 zircon grains) and Potosí deposits (17 zircon grains), respectively. Chromitite samples were crushed to a grain size <125 μm using a RETSCH vibratory disc mill (RS 100) equipped with an agate grinding set. A rough pre-concentration was achieved by ultrasonic decantation followed by a carefully performed wet sieving by hand through standard screen series (53, 75, 106, 125 μm). The <53 μm and 53–75 μm fractions were processed by hydroseparation, using the computer-controlled device CNT HS 11 at the HS laboratory in Barcelona (see Aiglsperger et al., 2015 for technical details; www.hslab-barcelona.com). The separation process was accomplished with ascending flow rates and changing impulse regimes in two steps: (1) production of a preliminary concentrate using a 30 cm long glass separation tube (GST) (inner diameter 8 mm); (2) production of the final concentrate using a 10 cm long GST (inner diameter 5 mm). Several monolayer polished sections (2.5 cm) were produced from 0.2 mg of each final concentrate, which were later analyzed by optical and scanning electron microscope (SEM) at the University of Barcelona.

3.3. Mineral imaging

Prior to the isotopic analyses all zircon grains were imaged by Cathodoluminescence (CL) and/or Backscatered Electron (BSE)

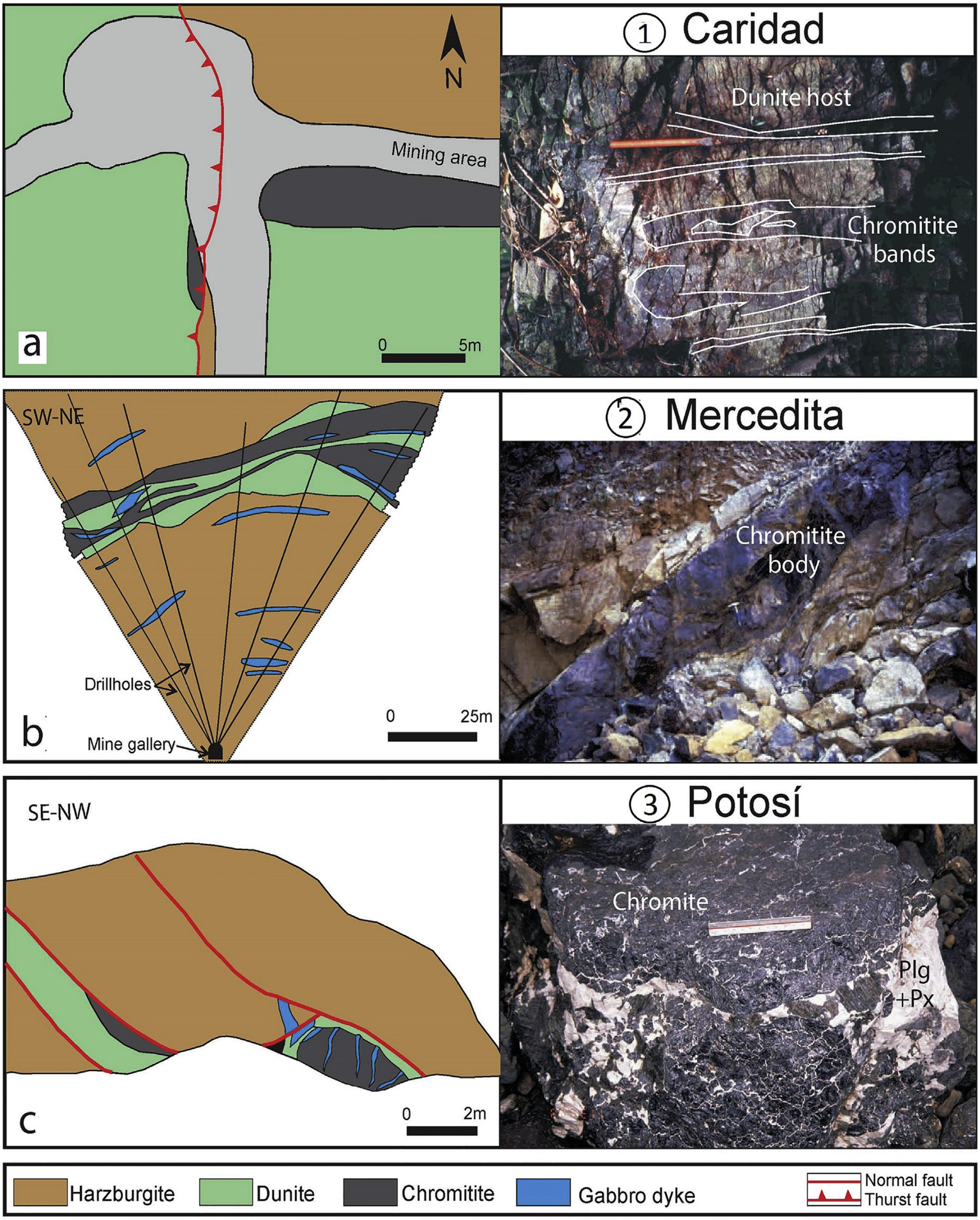

Figure 2. Field sketches (a, c), vertical cross section (b) and field photographs showing morphologies and structures of the studied chromitite deposits: Caridad, Mercedita (modified from Proenza et al., 1998, 1999), Potosí (modified from Proenza et al., 2001a).

mode to examine their internal structure. CL and BSE images of the zircon grains were obtained using two Scanning Electron Microscopes (SEM): (1) a Zeiss EVO MA15 at the Geochemical Analysis Unit (GAU) of the GEMOC/CCFS Centre in the Department of Earth and Planetary Sciences, Macquarie University, Sydney; and (2) an Environmental SEM Quanta 200 FEI, XTE 325/D8395 equipped with an INCA Energy 250 EDS microanalysis system at the University of Barcelona.

Table 1
Zircon U-Pb age data for the chromitites from the Mayarí-Baracoa Ophiolitic Belt, eastern Cuba.

Analysis no.	Isotope ratios							
	$^{207}Pb/^{206}Pb$	$\pm 2\sigma$	$^{207}Pb/^{235}U$	$\pm 2\sigma$	$^{206}Pb/^{238}U$	$\pm 2\sigma$	$^{208}Pb/^{232}Th$	$\pm 2\sigma$
SHRIMP data								
caridad								
Zr-1	0.06392	0.00871	0.79111	0.11626	0.08976	0.00493	0.02699	0.00242
Zr-2	0.11416	0.00370	4.65272	0.27745	0.29559	0.01480	0.07062	0.01926
Zr-3	0.12691	0.00184	6.28703	0.27892	0.35931	0.01507	0.09442	0.00455
Zr-4	0.12828	0.00121	6.56759	0.28506	0.37133	0.01573	0.09922	0.00756
Zr-5	0.13243	0.00275	6.65594	0.31937	0.36452	0.01576	0.10018	0.00559
LA-(MC)-ICPMS data								
Mercedita								
Zr-6	0.0524	0.0031	0.3312	0.0193	0.0458	0.0014	0.01399	0.00162
Zr-7	0.0514	0.0036	0.3266	0.0221	0.0461	0.0015	0.01463	0.00142
Zr-8	0.0626	0.0087	0.4108	0.0536	0.0476	0.0028	0.08215	0.02165
Zr-9	0.0593	0.0036	0.4034	0.0243	0.0493	0.0016	0.01556	0.00171
Potosí								
Zr-10	0.1445	0.0725	0.3096	0.1416	0.0155	0.0033	0.01026	0.00471
Zr-11	0.0728	0.0143	0.1859	0.0346	0.0185	0.0012	0.00866	0.00227
Zr-12C	0.0513	0.0018	0.3223	0.0113	0.0456	0.0011	0.01442	0.00072
Zr-12R	0.0520	0.0015	0.3209	0.0098	0.0447	0.0011	0.01397	0.00062
Zr-13	0.0524	0.0015	0.3315	0.0104	0.0459	0.0011	0.01472	0.00084
Zr-14	0.0461	0.0068	0.2950	0.0427	0.0465	0.0014	0.01491	0.00066
Zr-15	0.0536	0.0020	0.3442	0.0125	0.0466	0.0011	0.01579	0.00104
Zr-16	0.0534	0.0027	0.3476	0.0185	0.0472	0.0015	0.01520	0.00168
Zr-17	0.0528	0.0022	0.3448	0.0141	0.0474	0.0012	0.01508	0.00116
Zr-18	0.0528	0.0024	0.3561	0.0172	0.0490	0.0016	0.01741	0.00178
Zr-19	0.0586	0.0021	0.3991	0.0154	0.0494	0.0014	0.01636	0.00112
Zr-20C	0.0621	0.0017	0.9979	0.0291	0.1166	0.0028	0.03643	0.00188
Zr-20R	0.0623	0.0023	1.0097	0.0378	0.1175	0.0030	0.03778	0.00272
Zr-21	0.0625	0.0017	1.0081	0.0298	0.1170	0.0029	0.03586	0.00202
Zr-22	0.0705	0.0020	1.4518	0.0463	0.1495	0.0040	0.04510	0.00264
Zr-23	0.1220	0.0033	6.0456	0.1883	0.3597	0.0096	0.08606	0.00476
Zr-24	0.1263	0.0033	5.9458	0.1655	0.3415	0.0081	0.09718	0.00488
Zr-25	0.1321	0.0040	6.5554	0.2240	0.3600	0.0101	0.10444	0.00682
Zr-26C	0.1909	0.0067	14.0474	0.5292	0.5339	0.0150	0.13871	0.01134
Zr-26R	0.1547	0.0063	9.1525	0.4007	0.4291	0.0130	0.12339	0.01252

3.4. U-Pb and Hf isotopes

Zircon grains were analyzed *in situ* for U–Pb and Hf isotopes, using a LA-ICPMS and a LA-MC-ICPMS, respectively, at the Geochemical Analysis Unit (GAU) of the GEMOC/CCFS (Sydney, Australia). Moreover, five zircon grains with grain-sizes less than 60 μm were dated using a SHRIMP II instrument, in the John de Laeter Centre, Curtin University (Perth, Australia). The results are listed in Tables 1 and 2. Further details of the analytical methods for isotopic analyses and calculations (e.g. ε_{Hf}, T_{DM}) are given in Appendix 1.

4. Results

4.1. The Caridad chromite deposit

The zircon crystals are mainly stubby, vary in shape from euhedral (equant) to broken crystals and are about 50 μm across (Fig. 3). The cathodoluminescence (CL) images show the presence of cloudy oscillatory zoning, in one case with signs of magmatic resorption and overgrowth (Zr-3 in Fig. 3). The exception is grain Zr-1, which is a broken crystal with sector zoning parallel to crystal faces. All zircon grains are free of mineral inclusions, except grain Zr-2 which shows a highly- luminescent euhedral core related to monazite. Ion microprobe analyses of these zircon grains ($n = 5$) yield concordant Neoproterozoic ages (554 ± 29 Ma; 2σ uncertainty) and mainly subconcordant Paleoproterozoic ages (1867 ± 58 Ma to 2130 ± 36 Ma) (Fig. 3, Table 1 and Appendix 2). The Neoproterozoic zircon grain shows highly unradiogenic Hf-isotope ratios ($\varepsilon_{Hf}(t) = -26.5$) corresponding to a 2.14 Ga depleted-mantle Hf model age (T_{DM}), whereas the Paleoproterozoic grains show a restricted range of Hf-isotope compositions ($\varepsilon_{Hf}(t) = -3.2$ to $+0.9$) close to that of contemporary depleted upper mantle and T_{DM} from 2.34 to 2.62 Ga (Fig. 3; Table 2).

4.2. The Mercedita chromite deposit

The four grains recovered from the chromitite sample are euhedral in shape with elongated habits (Fig. 4). All zircon grains are characterized by oscillatory zoning parallel to the external faces of the crystal. Two zircon grains (Zr-6 and Zr-8) contain minute inclusions of monazite (Fig. 4). *In situ* LA-ICP-MS analyses of the zircon ($n = 4$) yield concordant U-Pb early Permian and late Carboniferous ages between 289 ± 9 Ma and 310 ± 10 Ma, with a lower intercepts at 290 ± 8 Ma (Table 1 and Appendix 2). These Paleozoic zircon grains exhibit $\varepsilon_{Hf}(t)$ between −5.57 and −3.67, and T_{DM} ranges from 1.07 Ga to 1.15 Ga (Fig. 4, Table 2).

4.3. The Potosí chromite deposit

The zircon crystals recovered from the Potosí chromite deposit vary in shape from euhedral (elongated to equant) to rounded, and in some cases have convolute or oscillatory zoning and inherited cores overgrown by younger rims (Figs. 5–7). SEM-EDS and micro-Raman analyses reveal that many of these zircon grains host inclusions of K-feldspar, quartz, biotite and apatite, and occasional ilmenite (Figs. 6 and 7). Typical mantle minerals (olivine, orthopyroxene, clinopyroxene, Cr-spinel) where not found as inclusions in the zircon grains. There is no clear correlation between zircon shape, presence of mineral inclusions and age, although some of the oldest zircon grains are rounded (Figs. 6 and 7).

LA-MC-ICPMS analyses on 17 individual zircon grains yielded three age populations (Figs. 5–7, Table 1 and Appendix 2). The two

Ages (Ma)										Concentration (ppm)	
$^{207}Pb/^{206}Pb$	±2 σ	$^{207}Pb/^{235}U$	±2 σ	$^{206}Pb/^{238}U$	±2 σ	$^{208}Pb/^{232}Th$	±2 σ	Used age	±2 σ	Th	U
739	288			554	29	538	48	554	29		
1867	58			1669	74	1379	364	1867	58		
2056	26			1979	71	1824	84	2056	26		
2074	17			2036	74	1912	139	2074	17		
2130	36			2004	74	1930	103	2130	36		
303	130	291	15	289	9	281	32	289	9	2090	1569
261	155	287	17	290	9	294	28	290	9	203	319
693	282	349	39	300	17	1596	404	300	17	19	1038
579	129	344.1	18	310.4	10	312.1	34	310	10	780	929
2282	756	274	110	99	21	206	94	99	21	8	15
1009	374	173	30	118	8	174	46	118	8	15	47
253	80	284	8	287	6	289	14	287	6	287	344
287	66	283	8	282	6	280	12	282	6	890	729
301	68	291	8	290	8	295	16	290	8	1119	1837
0	328	263	34	293	8	299	14	293	8	833	302
353	84	300	10	294	6	317	20	294	6	330	452
345	118	303	14	297	10	305	34	297	10	527	1366
318	96	301	10	299	8	303	24	299	8	386	444
318	104	309	12	308	10	349	36	308	10	1399	4237
552	78	341	12	311	8	328	22	311	8	958	768
678	60	703	14	711	16	723	36	711	16	372	621
686	80	709	20	716	18	750	52	716	18	145	283
691	58	708	16	713	16	712	40	713	16	193	1283
941	58	911	20	898	22	892	52	898	22	440	1224
1985	50	1982	28	1981	46	1669	88	1985	50	413	381
2047	48	1968	24	1894	38	1875	90	2047	48	275	223
2126	54	2053	30	1982	48	2008	124	2126	54	764	743
2750	60	2753	36	2758	64	2625	202	2750	60	543	342
2398	72	2353	40	2302	58	2352	226	2398	72	329	1546

Table 2
Zircon Hf-isotope data for the chromitites from the Mayarí-Baracoa Ophiolitic Belt, eastern Cuba.

Analysis No.	Measured Lu-Hf ratios				$Hf_{initial}$	$\varepsilon_{Hf}(t)$	±SE	T_{DM} (Ga)	$T_{DM}^{Crustal}$ (Ga)	Used age (Ma)	±2 σ
	$^{176}Hf/^{177}Hf$	±SE	$^{176}Lu/^{177}Hf$	$^{176}Yb/^{177}Hf$							
Caridad											
Zr-1	0.281689	0.000052	0.000121	0.003787	0.281688	−26.5	1.8	2.14	2.96	554	29
Zr-2	0.281580	0.000029	0.001030	0.033808	0.281544	−1.8	1.0	2.34	2.59	1867	58
Zr-3	0.281553	0.000043	0.001443	0.041571	0.281497	0.9	1.5	2.41	2.59	2056	26
Zr-4	0.281480	0.000032	0.001204	0.036911	0.281433	−1.0	1.1	2.49	2.71	2074	17
Zr-5	0.281369	0.000036	0.000891	0.024622	0.281333	−3.2	1.3	2.62	2.89	2130	36
Mercedita											
Zr-6	0.282495	0.000019	0.002533	0.071026	0.282481	−4.30	0.67	1.12	1.46	289	9
Zr-7	0.282507	0.000024	0.001483	0.063597	0.282499	−3.67	0.85	1.07	1.43	290	9
Zr-8	0.282493	0.000008	0.001156	0.042541	0.282487	−4.11	0.27	1.08	1.45	300	17
Zr-9	0.282455	0.000013	0.001794	0.064364	0.282445	−5.57	0.46	1.15	1.54	310	10
Potosí											
Zr-10	0.283095	0.000022	0.000493	0.018789	0.283094	13.50	0.78	0.22	0.27	99	21
Zr-12C	0.282489	0.000010	0.000988	0.027823	0.282484	−4.3	0.3	1.08	1.46	287	6
Zr-13	0.282516	0.000012	0.000756	0.021382	0.282512	−3.2	0.4	1.04	1.40	290	8
Zr-14	0.282600	0.000011	0.002824	0.081350	0.282585	−0.6	0.4	0.97	1.25	293	8
Zr-16	0.282734	0.000030	0.001740	0.049026	0.282724	4.5	1.1	0.75	0.95	297	10
Zr-17	0.282475	0.000012	0.001213	0.036942	0.282468	−4.6	0.4	1.11	1.48	299	8
Zr-18	0.282516	0.000019	0.000971	0.029564	0.282510	−2.9	0.7	1.04	1.39	308	10
Zr-19	0.282508	0.000017	0.000999	0.027834	0.282502	−3.1	0.6	1.05	1.41	311	8
Zr-20C	0.282704	0.000024	0.001226	0.031482	0.282688	12.4	0.8	0.78	0.82	711	16
Zr-20R	0.282608	0.000024	0.000554	0.015064	0.282601	9.5	0.8	0.90	1.00	716	18
Zr-21	0.282718	0.000022	0.000064	0.002000	0.282717	13.5	0.8	0.74	0.75	713	16
Zr-22	0.281999	0.000018	0.000505	0.016019	0.281990	−8.0	0.6	1.74	2.17	898	22
Zr-23	0.281294	0.000016	0.000994	0.034733	0.281257	−9.3	0.6	2.73	3.13	1985	50
Zr-24	0.281400	0.000022	0.000374	0.011537	0.281385	−3.3	0.8	2.55	2.83	2047	48
Zr-25	0.281461	0.000012	0.000385	0.011058	0.281445	0.7	0.4	2.47	2.66	2126	54
Zr-26C	0.281042	0.000029	0.000790	0.021452	0.281000	−0.6	1.0	3.06	3.23	2750	60
Zr-26R	0.281224	0.000023	0.000219	0.005600	0.281214	−1.2	0.8	2.77	2.99	2398	72

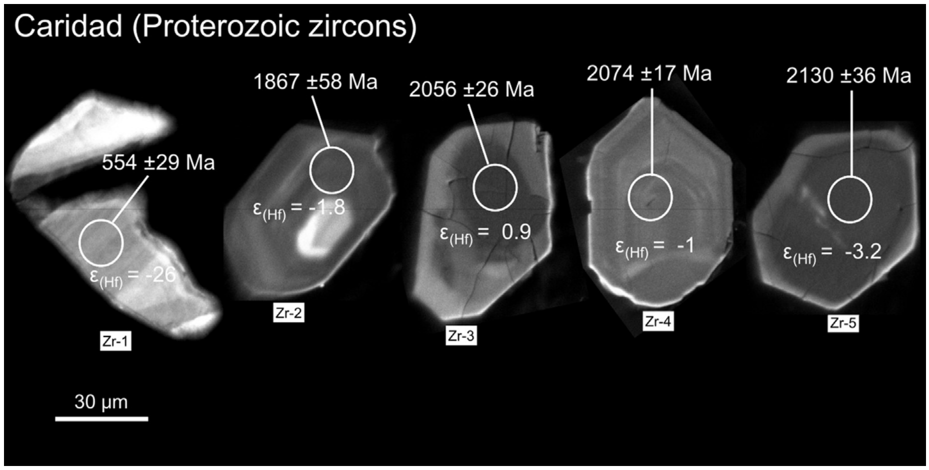

Figure 3. CL images of Proterozoic zircon grains from the chromitites of Caridad deposit, eastern part of Mayarí-Cristal Ophiolitic Massif (Sagua de Tánamo area).

euhedral inclusion-free zircon grains (Zr-10 and Zr-11) yielded concordant Cretaceous ages of 99 ± 21 Ma and 118 ± 8 Ma (2σ uncertainty), respectively (Fig. 5). LA-MC-ICPMS analysis of Zr-10 yielded a radiogenic Hf-isotope ratio ($\varepsilon_{Hf}(t) = +13.5$) and T_{DM} age of 0.22 Ga. The other zircon grains yielded Permian-Carboniferous (282 ± 6 Ma to 311 ± 8 Ma), Neoproterozoic (711 ± 16 Ma to 898 ± 22 Ma), and Paleoproterozoic (1985 ± 50 Ma to 2126 ± 54 Ma) ages (Figs. 6 and 7). One zircon (Zr-26; Fig. 7) has an inherited core of Neoarchean age (2750 ± 60 Ma) surrounded by a cloudy Paleoproterozoic (2397 ± 72 Ma) rim. In general, these zircon grains show $\varepsilon_{Hf}(t)$ between −9 and −0.6 (T_{DM} = 0.97 to 3.06 Ga), but 4 grains exhibit $\varepsilon_{Hf}(t)$ more radiogenic than the contemporaneous chondritic upper mantle (Carboniferous Zr-16 = +4.5, Neoproterozoic Zr-20 = +9.5 to +12.4 and Zr-21 = +13.5, and Paleoproterozoic Zr-25 = +0.7) (Figs. 6 and 7 and Table 1). Hf model ages of the zircon grains with positive $\varepsilon_{Hf}(t)$ range from 0.74 to 2.47 Ga (Table 2).

5. Discussion

5.1. Origin of zircon grains in the eastern Cuban ophiolitic chromitites

Zircon grains from the eastern Cuba chromitites yield a significant range in age, scattering from Cretaceous (99 Ma) to Neoarchean (2750 Ma) with $\varepsilon_{Hf}(t)$ values ranging from −26.5 to +13.5. The youngest ages (99 and 118 Ma) coincide with the formation age of the oceanic crust of the hosting ophiolite while the older zircon grains are considered to be inherited (Fig. 8). Below we discuss the possible origin of these zircon grains.

5.1.1. Cretaceous zircon grains related to ophiolite formation

Two zircon grains (Zr-10 and Zr-11; Fig. 5, Table 1) from the Potosí chromite deposit are essentially of the same age (99 and 118 Ma) as zircon grains of igneous rocks related to ophiolite formation (90–125 Ma; Iturralde-Vinent, 1996; Iturralde-Vinent et al., 2006). The ages of these zircon grains match, within uncertainty, the U-Pb age of zircon grains from a Fe-Ti-rich gabbro intruding the mantle peridotite section at the Moa-Baracoa ophiolitic massif (124 ± 1 Ma; Rojas-Agramonte et al., 2016). Cretaceous zircon grains in the gabbro were interpreted to date the time of crystallization, and therefore of ophiolite formation. The corresponding mean $\varepsilon_{Hf}(t)$ value of +13 in these zircon grains (Rojas-Agramonte et al., 2016) is identical to the Cretaceous zircon of the Potosí chromite deposit ($\varepsilon_{Hf}(t) = +13.5$) suggesting that both derived from a juvenile (mantle) source (Figs. 5 and 9). Indeed, the euhedral morphology of the chromitite-hosted zircon and its juvenile Hf-isotopic composition (Fig. 5) indicate a genetic link between zircon crystallization, the host chromitite, and the overlying crustal

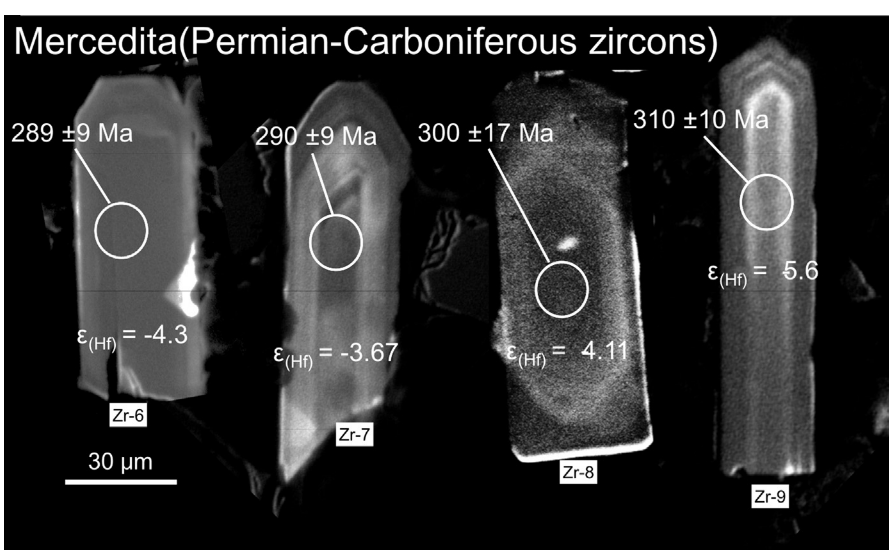

Figure 4. CL images of Permian–Carboniferous zircon grains from the chromitites of Mercedita deposit, Moa-Baracoa Ophiolitic Massif.

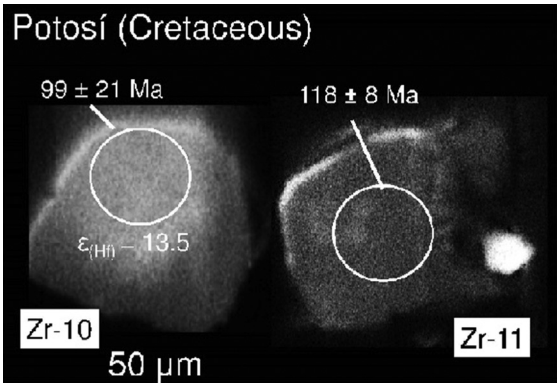

Figure 5. BSE images of Cretaceous zircon grains from the chromitites of Potosí deposit, Moa-Baracoa Ophiolitic Massif.

igneous rocks. In this scenario, the zircon age of 99 Ma would provide a minimum age for chromitite crystallization in the mantle just below the Moho, from melts migrating upwards to the developing oceanic crust. However, Proenza et al. (2001a) noted that the Potosí chromitites were intruded by different pegmatitic mafic dykes (Figs. 1d and 2c) that produced brecciation, partial dissolution, and recrystallization of chromitite. According to these authors, Ti- and Zr-bearing minerals such as Mg-rich ilmenite, baddeleyite and zirconolite were found in the contact zone between chromitite and associated mafic dykes. Although not dated yet, these mafic dykes also contain zircon grains as well as other HFSE-bearing minerals, indicative of their crystallization from highly evolved hydrated basaltic melts rich in Fe-Ti (Proenza et al., 2001a, b). This leads us to suggest the possibility that Cretaceous zircon grains recovered from the Potosí chromitite sample could have crystallized from the intruding mafic melts that overprinted the chromitite body instead of being co-genetic with the chromitite. In this latter scenario, these zircon grains could be dating the timing of late episodes of intrusion of basaltic magmas associated with ophiolite formation. Gabbroic dikes intruding harzburgite and dunite in the MTZ are a characteristic feature of ophiolitic complexes (e.g., Kelemen et al., 1997).

5.1.2. Inherited zircon grains with negative $\varepsilon_{Hf}(t)$ (continental crust zircon grains)

Most of the recovered inherited zircon grains (20 grains) from the three chromitite bodies have negative $\varepsilon_{Hf}(t)$ (Table 1), suggesting they are derived from old continental crust and variably contaminated upper mantle source regions. Most of these zircon grains are of Permo-Carboniferous age (287–311 Ma; $\varepsilon_{Hf}(t) = -5.6$ to -0.6; Figs. 4 and 6). The remaining age populations include mainly Neoproterozoic (554–898 Ma; $\varepsilon_{Hf}(t) = -26.5$ to -8.0; Zr-1 in Fig. 3 and Zr-22 in Fig. 7), Paleoproterozoic (1867–2397 Ma; $\varepsilon_{Hf}(t) = -9.3$ to -1; Figs. 3 and 7), and one Neoarchean zircon grain (2750 Ma; $\varepsilon_{Hf}(t) = -0.6$; Zr-26 in Fig. 7). The age ranges of these zircon grains broadly match, in terms of ages and Hf isotopic systematics, with inherited zircon grains of continental crust origin found in the Cretaceous supra-subduction zone ophiolitic and volcanic arc rocks of Cuba (~135–70 Ma; Rojas-Agramonte et al., 2010, 2016; Figs. 8 and 9). This suggests that zircon grains in the mantle-hosted chromitite and the igneous rocks of the overlying crust probably were derived from the same crustal source. This is consistent with the fact that many of the chromitite-hosted zircon grains, regardless of their morphology, internal structure, age and Hf isotopic composition, contain inclusions of crustal minerals, such as quartz, K-feldspar, biotite and apatite (Figs. 6 and 7) and lack inclusions of typical mantle minerals such as olivine, pyroxene and Cr-spinel. Hence, crustally-derived zircon grains may have been introduced into the mantle by subduction of detrital sediments deposited on the ocean floor or the trench and/or by subduction erosion of sediments deposited on the fore-arc (e.g. Yamamoto et al., 2013; Rojas-Agramonte et al., 2016). They could have been physically transported into the mantle wedge beneath the Greater Antilles paleo-volcanic arc by fluids or melts, that likely penetrated the mantle wedge along brittle (veins) or ductile (diapirs/cold plumes) structures (Castro et al., 2010; Marschall and Schumacher, 2012; Spandler and Pirard, 2013). This interpretation is consistent with the Pb isotopic systematics of igneous rocks from eastern Cuba, which fingerprint subducted Atlantic (North American-derived) sediments within the subduction factory of the Greater Antilles Paleo-arc (Marchesi et al., 2007).

We propose that pre-existing (inherited) zircon grains with negative $\varepsilon_{Hf}(t)$, document crustal contamination of the supra-subduction oceanic mantle. They resided in the mantle peridotite and underwent no significant resetting of their U-Pb ages despite the high temperature of the mantle (Stern et al., 2010 and references therein), before being entrained into the chromitite bodies (Yamamoto et al., 2013).

5.1.3. Inherited zircon grains with positive $\varepsilon_{Hf}(t)$: SCLM or continental crust zircon grains?

The eastern Cuba chromitites also contain 5 inherited zircon grains (Potosí: Zr-16, Zr-20, Zr-21, Zr-25; Caridad: Zr-3; Figs. 3, 6 and 7 and Table 2) with positive $\varepsilon_{Hf}(t)$ (+0.7 to +13.5), typical of zircon grains that crystallized from melts derived from a juvenile (mantle) sources. In particular, two Neoproterozoic (711 and 713 Ma) zircon grains from Potosí (Zr-20 and Zr-21, Fig. 7) have a remarkably mantle-like Hf isotope signature $\varepsilon_{Hf}(t)$ ranging from +12.4 to +13.5, and mean T_{DM} of 0.76 Ga. In principle, these zircon grains with Hf-isotope composition, indicative of mantle-derived melts, could be grains that originally crystallized in a portion of ancient subcontinental lithosphere mantle (SCLM), or grains that were incorporated into the mantle wedge of the Great Antilles Paleo-arc by subduction of detrital sediments derived from rocks that have crystallized from melts with juvenile sources (e.g., mafic to intermediate igneous rocks).

It is important to note that platinum-group minerals (PGM) and base-metal sulfides (BMS) in chromitite bodies of eastern Cuba give a range of Os model ages ($T_{MA} \approx T_{RD}$) from 0.1 to 1.2 Ga, suggesting the presence of different ancient depleted domains in the mantle wedge beneath the Greater Antilles paleo-island arc (Marchesi et al., 2011; González-Jiménez et al., 2012). These Os model ages suggest that the protoliths of chromitite-bearing MBOB mantle section may be derived from ancient SCLM as old as Proterozoic, as described in ophiolites elsewhere (Peltonen et al., 2003; Shi et al., 2007; McGowan et al., 2015).

As noted above, the Potosí chromitites contain two Neoproterozoic zircon grains (~700 Ma) with remarkably positive $\varepsilon_{Hf}(t)$ (+12.4 to +13.5). Considering the uncertainties inherent in model age calculations, the Hf model ages (T_{DM} of 0.76 Ga) of these zircon grains overlap to the Os model ages of 0.72 and 0.75 Ga obtained by Marchesi et al. (2011) and González-Jiménez et al. (2012) in PGM and BMS populations of Mayarí-Baracoa chromitites. This age match may indicate the existence of a Proterozoic mantle precursor (protolith), which experienced melting events during Neoproterozoic time, in the mantle wedge beneath the Greater Antilles paleovolcanic arc. Thus the two Proterozoic zircon grains with $\varepsilon_{Hf}(t) \gg 0$ could provide support for the hypothesis that residual domains of ancient SCLM as old as Proterozoic of likely Gondwana affinity were present within the Caribbean lithosphere (Kamenov et al., 2011), and served as platform for the construction

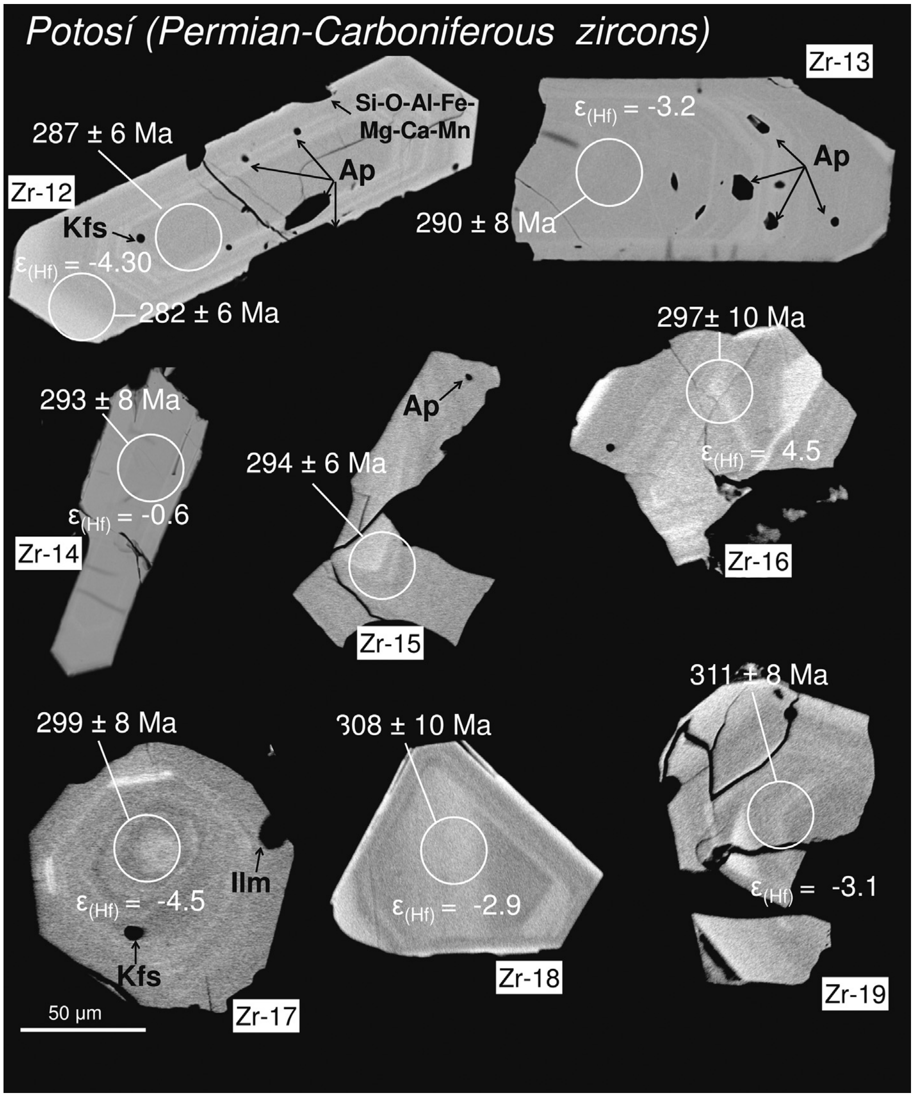

Figure 6. BSE images of Permian–Carboniferous zircon grains from the chromitites of Potosí deposit, Moa-Baracoa Ophiolitic Massif.

of the Cretaceous ophiolites (e.g., Shi et al., 2007; Griffin et al., 2009; O'Reilly et al., 2009; Tang et al., 2013).

However, other lines of evidence indicate that the zircon grains with positive $\varepsilon_{Hf}(t)$ were not crystallized from the melts/fluids in the mantle: (1) the zircon grains are well-rounded grains without overgrowths (Zr-20 and Zr-21, Fig. 7) suggesting mechanical abrasion during sedimentary transport; (2) the common occurrence of Permo-Carboniferous and Neoproterozoic terranes with similar $\varepsilon_{Hf}(t)$ values of −20 to +15 in the margin of Proto-Caribbean basin (e.g., Cardona et al., 2010; Kirsch et al., 2012; Cochrane et al., 2014; Ortega-Obregón et al., 2014; Solari et al., 2014; Fig. 9). According to these observations, subduction of detrital material might account for the presence of inherited zircon grains with positive $\varepsilon_{Hf}(t)$. Zircon grains from continental crust can also have juvenile Hf isotope signatures (e.g., zircon grains from I-type relatively mafic granitoids such as tonalite and granodiorite). These zircon grains survived melting of recycled continental crust (e.g. Rojas-Agramonte et al., 2016) in a single process (cycle) of erosion, deposition, subduction and transfer into the mantle.

We favor the idea that inherited zircon grains with positive $\varepsilon_{Hf}(t)$ were incorporated into the mantle wedge either after subduction of detrital sediments or from remnants of ancient SCLM (Gondwana-derived) left behind during the fragmentation of Pangea at the oceanic Proto-Caribbean lithospheric mantle.

5.2. Comparison with ancient xenocrystic zircon grains from other mantle-hosted ophiolitic chromitites

Dated zircon grains interpreted as xenocrysts have been reported from mantle-hosted chromitites of the Ray–Iz ophiolite (Polar Urals, Russia; Savelieva et al., 2007; Robinson et al., 2015), Luobusa ophiolite (southern, Tibet; Yamamoto et al., 2013; Robinson et al., 2015), Dongqiao ophiolites (central Tibet; Robinson et al., 2015), Oman ophiolite (Robinson et al., 2015), Dobromirtsi ophiolite (Bulgaria, González-Jiménez et al., 2015), SW Anatolian ophiolites (Turkey, Akbulut et al., 2016), and the Tumut ophiolite (southeast Australia, Belousova et al., 2015).

In general, U–Pb ages of zircon grains separated from ophiolitic chromitites are older than the host ophiolite (Yamamoto et al., 2013; Robinson et al., 2015; Akbulut et al., 2016; Belousova et al., 2015; this study). Systematically, zircon grains documented in ophiolitic chromitites mainly contain continental crust-derived mineral inclusions (quartz, K-feldspar and biotite), by contrast,

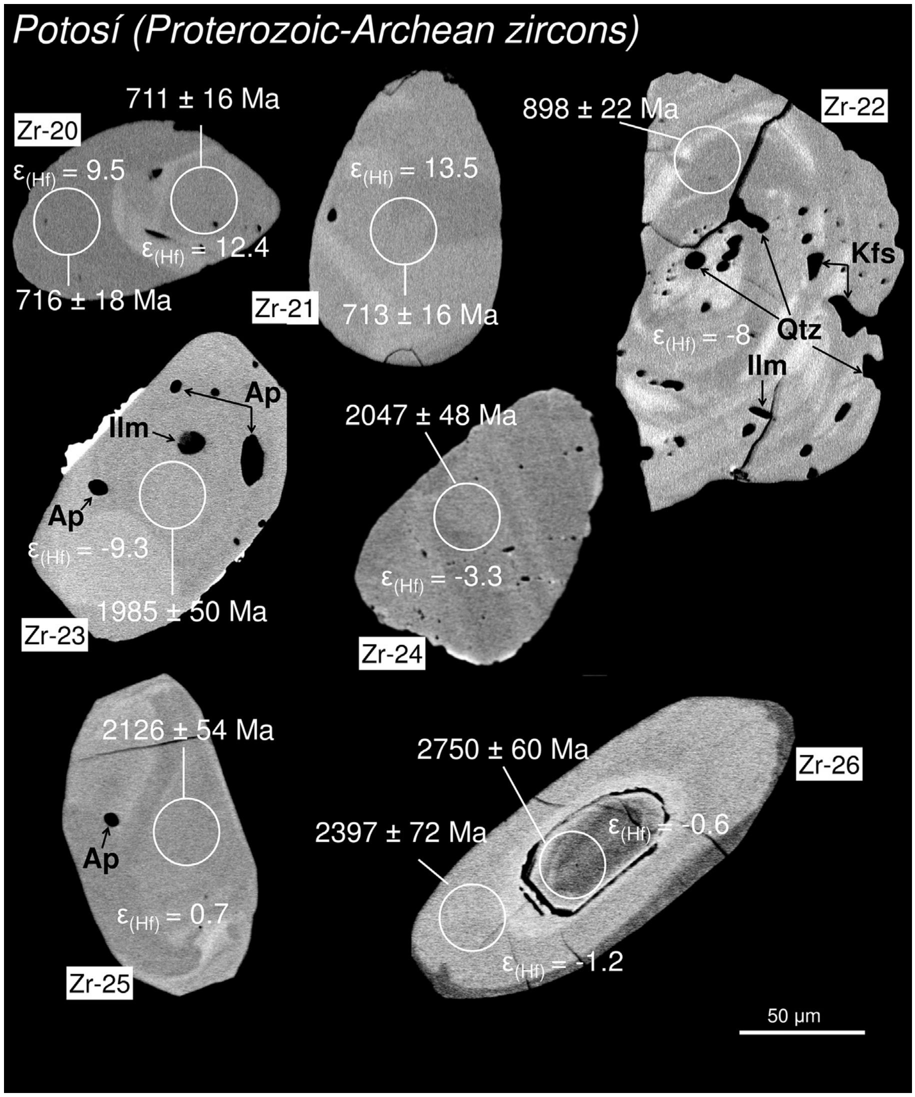

Figure 7. BSE images of Proterozoic and Archean zircon grains from the chromitites of Potosí deposit, Moa-Baracoa Ophiolitic Massif.

mantle minerals (olivine, orthopyroxene, clinopyroxene, Cr-spinel) have not been identified (Yamamoto et al., 2013; Robinson et al., 2015; Figs. 6 and 7 in this study).

The morphology of zircon crystals from ophiolitic chromitites varies from euhedral to subhedral and well-rounded. Some grains show oscillatory zoning parallel to external faces of the crystal (Savelieva et al., 2007; Yamamoto et al., 2013; Robinson et al., 2015; Fig. 4 in this study). However, many zircon grains occur as subangular to rounded grains suggesting a detrital history (Yamamoto et al., 2013; Robinson et al., 2015; Belousova et al., 2015; Griffin et al., 2016; Fig. 7 in this study).

Available studies reveal that zircon grains from ophiolitic mantle chromitites show a relatively restricted range of Hf isotope compositions. 376 $\pm$ 7 Ma euhedral zircon grains from Tibetan chromitites have $\varepsilon_{Hf}(t)$ of 8.5 $\pm$ 5.4 (McGowan et al., 2015). Two subhedral xenocrystic zircon grains (2257–1952 Ma) from Dobromirtsi chromitites have $\varepsilon_{Hf}(t) = -4.4$ to $+3.6$ (González-Jiménez et al., 2015). Seven rounded zircon grains (593–2289 Ma) recovered from Tumut ophiolite chromitites have $\varepsilon_{Hf}(t)$ values between -6 and $+6.8$ (Belousova et al., 2015). In contrast, zircon grains (99–2750 Ma) from eastern Cuba chromitites show a significant range in $\varepsilon_{Hf}(t)$ values (-26 to $+13.5$).

Previous studies have concluded that there is no correlation between age and morphology or internal structure (e.g., Yamamoto et al., 2013; Robinson et al., 2015). However, in general our results indicate that the younger zircon grains are mainly euhedral to subhedral crystals (Figs. 4–6), whereas older zircon grains are predominantly rounded grains (Fig. 7). Furthermore, the presence of euhedral zircon grains with pronounced oscillatory zoning did not crystallize from the magma that formed the chromitite bodies as they contain abundant inclusions of crustal minerals and clearly are xenocrysts (Fig. 6).

5.3. Provenance of inherited zircon grains

The LA-MC-ICPMS and SHRIMP analyses of zircon grains extracted from chromitite bodies of the Mayarí-Baracoa Ophiolite in eastern Cuba show a wide variation of ages and Hf-isotopic composition that broadly coincides with that found in inherited zircon grains of crustal origin in the Cretaceous Volcanic Arc and ophiolitic rocks of Cuba (Figs. 8 and 9; Rojas-Agramonte et al., 2016). These authors concluded that these zircon grains are xenocrysts recycled through the upper mantle within the Cretaceous subduction zone factory, and that most of them originated in

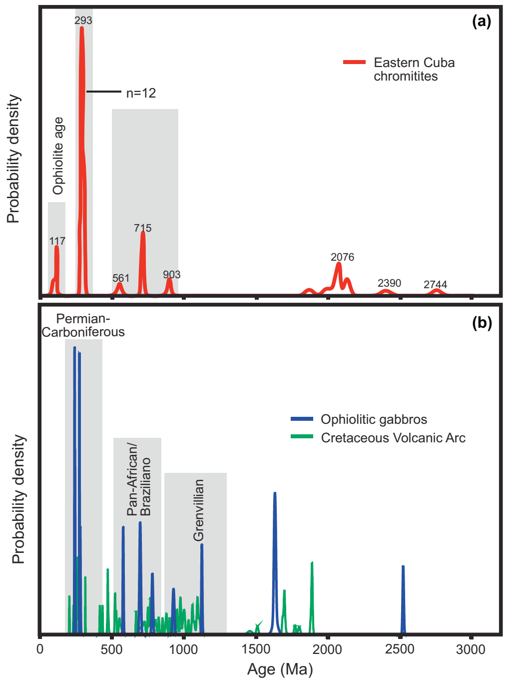

Figure 8. (a) Probability density plot showing U/Pb zircon ages of chromitites from Mayarí-Baracoa Ophiolitic Belt, eastern Cuba. (b) U/Pb ages of inherited zircon grains from the Cretaceous Volcanic Arc and ophiolitic rocks of Cuba (Rojas-Agramonte et al., 2016).

nearby exposed crustal terranes of northern South America and Central and North America (i.e., Chortis, Maya blocks and Mexican Terranes; Figs. 8–10).

The major population of zircon grains with Permian–Carboniferous ages in eastern Cuba chromitite samples could have been derived from Late Carboniferous–Permian plutonic rocks of the southwestern Mexico and Colombian Caribbean terranes, associated with a continental arc formed at the proto-Pacific margin (e.g., Keppie et al., 2004; Nance et al., 2006; Cardona et al., 2010; Leal-Mejía et al., 2011; Kirsch et al., 2012; Ortega-Obregón et al., 2014; Centeno et al., 2017). Derivation from the so-called East Mexico Arc in southern Mexico is supported by the predominant occurrence of zircon grains with ages from 287 to 311 Ma (Figs. 8 and 9). According to Kirsch et al. (2012), this magmatic continental arc includes deformed intrusive bodies (tonalite, diorite, granite, granodiorite, monzogranite, and subordinate hornblende-rich gabbro) with ages between *ca.* 280 and *ca.* 310 Ma. These intrusive bodies were rapidly exhumed to the surface by the end of Early Permian time (Kirsch et al., 2013). In the Colombian Andes, Late Carboniferous–Permian arc magmatism has been dated at 330–310 Ma (El Brage sector; Leal-Mejía et al., 2011), 275–260 Ma (Central Cordillera; Leal-Mejía et al., 2011), and 288–265 Ma (Santa Marta region; Cardona et al., 2010).

The Neoproterozoic inherited ages (554 ± 15 Ma to 898 ± 11 Ma, Panafrican/Braziliano) can possibly be related to terranes similar to those of southern Mexico (Talavera-Mendoza et al., 2005; Ortega-Obregón et al., 2014; Solari et al., 2014) and the palaeo-Pacific margin of the Gondwana supercontinent (Kemp et al., 2007). According to Rojas-Agramonte et al. (2016), Paleoproterozoic (1867 ± 29 Ma to 2126 ± 27 Ma) and Neoarchean (2750 ± 30 Ma) populations are mostly derived from "proto-Oaxaquia" terranes in SW Mexico (Weber and Schulze, 2014) and the palaeo-Pacific margin of the Gondwana supercontinent (Kemp et al., 2007).

5.4. Tectonic model

The evidence presented here indicates that the mantle wedge beneath the Early Cretaceous Antilles volcanic arc contained subducted continental-derived zircon grains. However, how can these xenocrystic zircon grains be transported and recycled into the shallow oceanic mantle? The origin of zircon grains, and other exotic minerals of typical crustal origin, in ophiolitic mantle

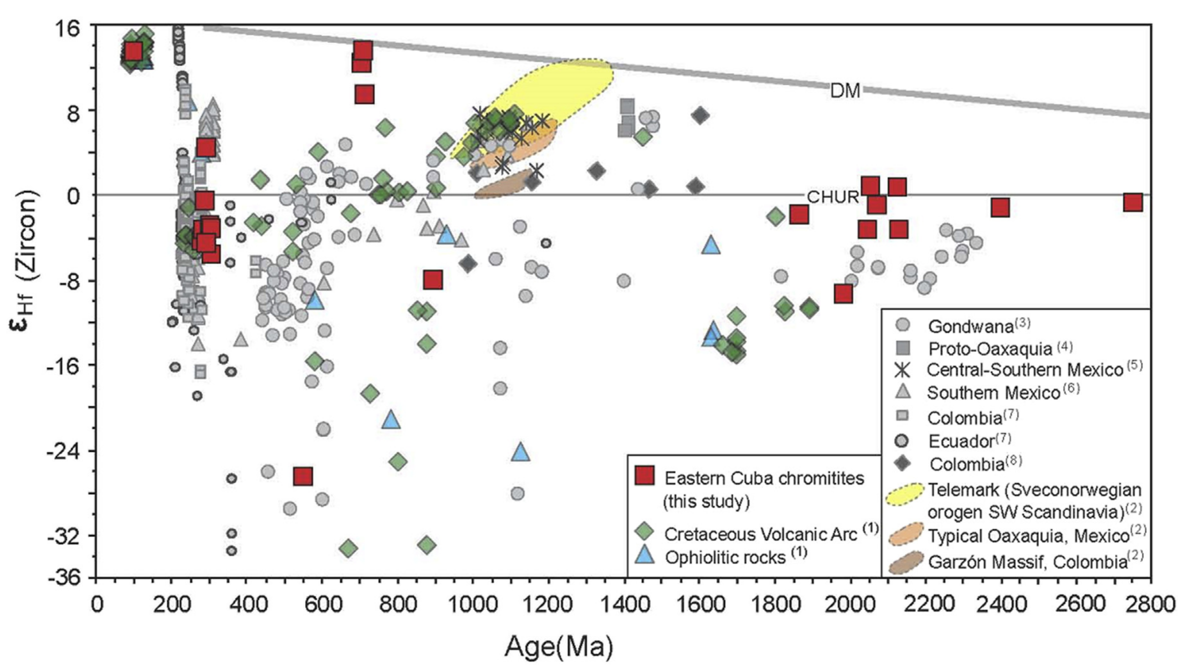

Figure 9. Plot of ε_{Hf} versus crystallization age for magmatic and inherited zircon grains of chromitites from Mayarí-Baracoa Ophiolitic Belt, eastern Cuba. For comparison U/Pb zircon ages of inherited zircon grains from the Cretaceous Volcanic Arc and ophiolitic rocks of Cuba; and sources of old detrital zircon in oceanic sediments entering trenches of the Cretaceous Caribbean arc system (Rojas-Agramonte et al., 2016).

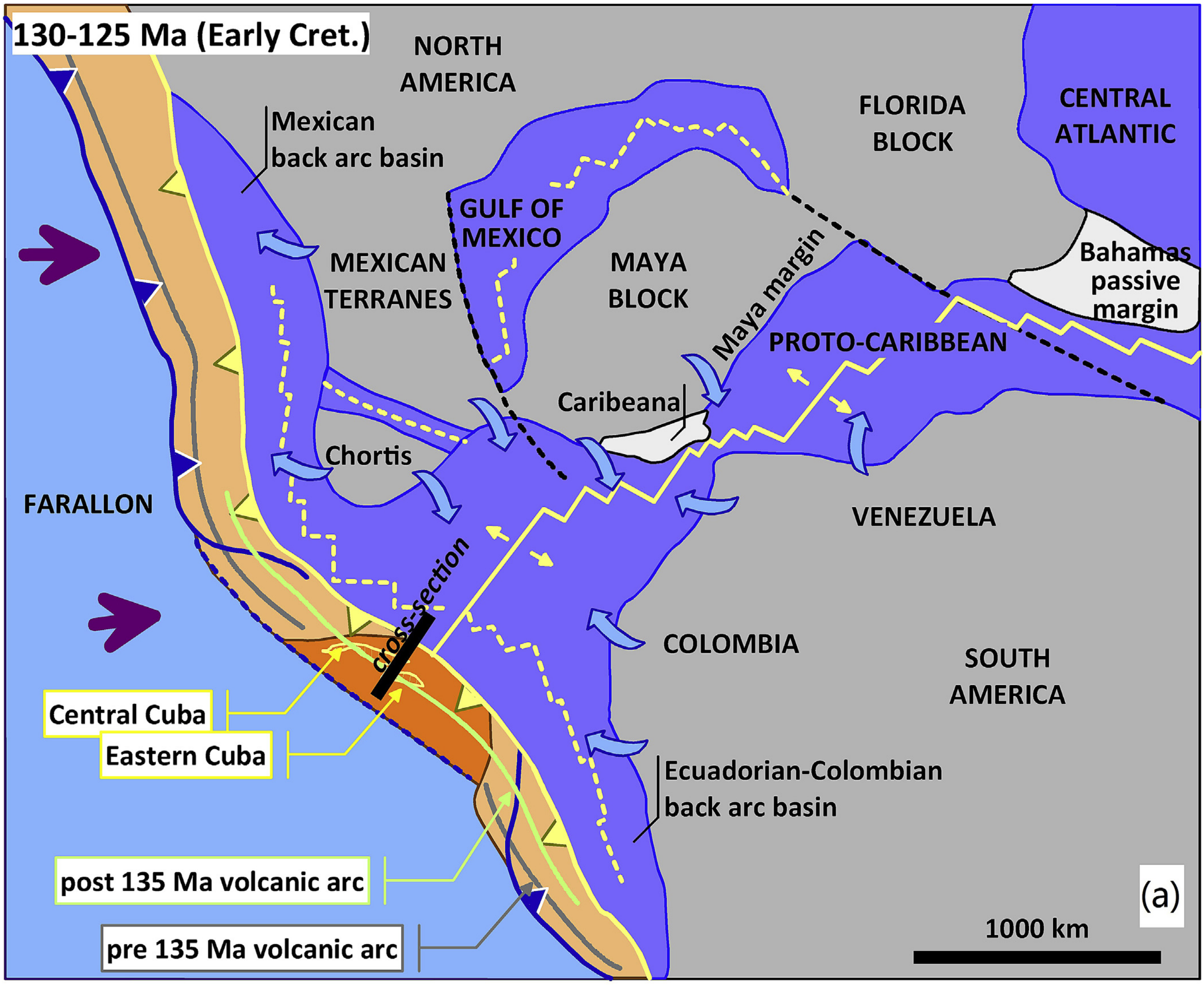

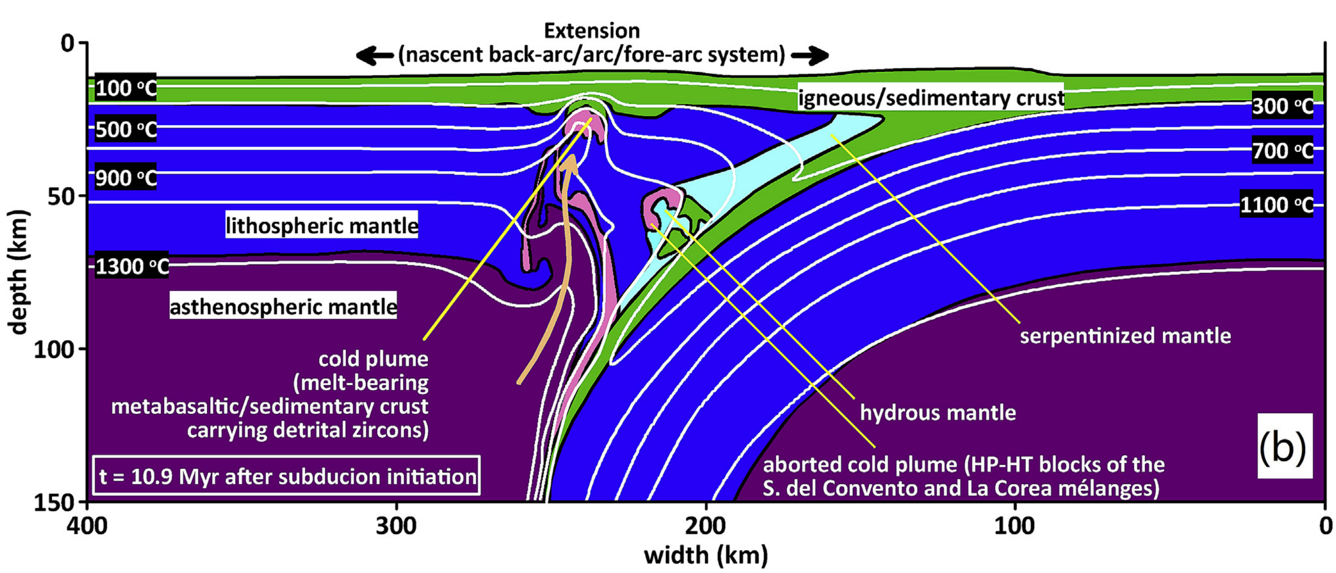

Figure 10. (a) Early Cretaceous geodynamic reconstruction of the Caribbean region (after Pindell and Kennan, 2009; Pindell et al., 2012; Boschman et al., 2014) showing flow of eroded North and South America detrital material towards basins (after Rojas-Agramonte et al., 2016) and of cross-section in Fig. 10b. (b) Numerical thermal-chemical model of ocean-ocean subduction of young (hot) oceanic lithosphere (age 10 million years; initial convergence rate of 4 cm/year) after Blanco-Quintero et al. (2011a). See text for explanation.

chromitites remains a hotly debated topic (Yamamoto et al., 2013; Zhou et al., 2014; Yang et al., 2014, 2015; Robinson et al., 2015; McGowan et al., 2015; Griffin et al., 2016). In general, models can be grouped into two broad categories: (1) transport of crustal material into the deep mantle (>420 km) by previous subduction processes, and zircon entrapment by a mantle plume (Yang et al., 2014, 2015); and (2) physical incorporation of zircon and other crustal minerals into the suprasubduction mantle wedge via subduction of oceanic crust, and later entrapment during formation of chromitite at low pressures in the shallow mantle (e.g., Zhou et al., 2014; Robinson et al., 2015).

In Fig. 10 the occurrence of crustally-derived xenocrystic zircon in mantle-hosted ophiolitic chromitites of eastern Cuba is conceptualized within the current models of plate tectonic evolution of the Caribbean region (Pindell et al., 2012; Boschman et al., 2014). Cretaceous spreading of the Proto-Caribbean ocean (connected with the central Atlantic) separated North and South America, while subduction of the young hot Proto-Caribbean lithosphere in the leading edge of the Farallon/Caribbean plate started in the Early Cretaceous (Rojas-Agramonte et al., 2011). The Moa ophiolite in eastern Cuba formed in the first 10–15 Ma after subduction initiation (Rojas-Agramonte et al., 2016; see also Lázaro et al., 2016; Torró et al., 2016, 2017) in a supra-subduction environment (Proenza et al., 1999, 2006; Gervilla et al., 2005; Marchesi et al., 2006, 2007), while ridge subduction formed partially-melted metabasaltic crust of the Sierra del Convento and La Corea mélanges (Garcia-Casco et al., 2006, 2008b; Lázaro et al., 2009; Blanco-Quintero et al., 2010, 2011a, b) interpreted as an aborted thermal-chemical cold plume formed at shallow depth (*ca.* 50 km, Blanco-Quintero et al., 2011a). An active partially molten thermal-chemical plume originating at greater depth from the subducted slab is indicated (Fig. 10). This cold plume comprises partially molten hydrated peridotite, dry solid mantle, and subducted oceanic crust (Gerya and Yuen, 2003; Gorczyk et al., 2007; Blanco-Quintero et al., 2011a), which may bear continental and juvenile detrital sediments derived from North and South America and containing zircon grains deposited in the Proto-Caribbean basin (Rojas-Agramonte et al., 2016; Torró et al., 2018). Ascent of these plumes from >100 km depth brings asthenospheric and lithospheric mantle and subducted crustal material to shallow mantle depths, contributing to arc magmatism (e.g., Castro et al., 2010) and the mineralogical/lithological heterogeneity of mantle wedges, including podiform chromitite-dunite bodies (Yamamoto et al., 2013; Zhou et al., 2014; Yang et al., 2014, 2015; Robinson et al., 2015; Griffin et al., 2016; González-Jiménez et al., 2017b).

6. Conclusions

(1) Zircon grains from chromitites in eastern Cuba ophiolites contain crustally-derived mineral inclusions (quartz, K-feldspar and biotite), but no inclusions of mantle minerals (olivine, orthopyroxene, clinopyroxene, Cr-spinel).
(2) Younger zircon grains are mainly euhedral to subhedral crystals, whereas older zircon grains are predominantly rounded grains. Most of the inherited zircon grains from the three chromitite bodies have negative $\varepsilon_{Hf}(t)$, suggesting their possible derivation from old continental crust and variably contaminated upper mantle source regions.
(3) Chromitite zircon grains are subducted detrital material incorporated into the mantle wedge beneath the Greater Antilles volcanic arc; they ultimately were derived from nearby exposed crustal terranes of northern part of South America and Mexico (i.e., Chortis, Maya blocks and Mexican terranes).
(4) Cold plumes offer a convincing explanation by which ancient zircon xenocrysts with a wide spectrum of ages and Hf isotopic compositions can be transferred to the mantle wedge above subducting slabs.

Acknowledgements

This research was financially supported by FEDER Funds, the Spanish Project CGL2015-65824 granted by the Spanish "Ministerio de Economía y Competitividad" to JAP, and the Ramón y Cajal Fellowship RYC-2015-17596 to JMGJ. This is also a contribution from the ARC National Key Centre for Geochemical Evolution and Metallogeny of Continents (www.es.mq.edu.au/GEMOC) and the ARC Centre of Excellence for Core to Crust Fluid Systems. Y.R-A acknowledges support by the Deutsche Forschungsgemeinschaft (DFG) grant RO4174/2-1. Support was also provided by the technical staff of the SHRIMP facility at Curtin University. Dr. Kristoffer Szilas, an anonymous referee, and Editorial Advisor of Geoscience Frontiers M. Santosh are deeply acknowledge for their constructive criticism that has helped to greatly improve the quality of the present manuscript.

Appendix A. Supplementary data

Supplementary data related to this article can be found at https://doi.org/10.1016/j.gsf.2017.12.005.

References

Aiglsperger, T., Proenza, J.A., Zaccarini, F., Lewis, J.F., Garuti, G., Labrador, M., Longo, F., 2015. Platinum group minerals (PGM) in the Falcondo Ni laterite deposit, Loma Caribe peridotite (Dominican Republic). Mineralium Deposita 50, 105–123.
Akbulut, M., González-Jiménez, J.M., Griffin, W.L., Belousova, E., O'Reilly, S.Y., McGowan, N., Pearson, N.J., 2016. Tracing ancient events in the lithospheric mantle: a case study from ophiolitic chromitites of SW Turkey. Journal of Asian Earth Sciences 119, 1–19.
Arai, S., 2013. Conversion of low-pressure chromitites to ultrahigh-pressure chromitites by deep recycling: a good inference. Earth and Planetary Science Letters 379, 81–87.
Bea, F., Fershtater, G.B., Montero, P., Whitehouse, M., Levin, V.Y., Scarrow, J.H., Austrheim, H., Pushkariev, E.V., 2001. Recycling of continental crust into the mantle as revealed by Kytlym Dunite zircons, Urals Mounts, Russia. Terra Nova 13, 407–412.
Belousova, E., González-Jiménez, J.M., Graham, I., Griffin, W.L., O'Reilly, S.Y., Pearson, N.J., Martin, L., Craven, S., Talavera, C., 2015. The enigma of crustal zircon grains in upper mantle rocks: clues from the Coolac ophiolite, SE Australia. Geology 43 (2), 119–122.
Blanco-Quintero, I.F., Garcia-Casco, A., Rojas-Agramonte, Y., Rodriguez Vega, A., Lázaro, C., Iturralde-Vinent, M.A., 2010. Metamorphic evolution of subducted hot oceanic crust, La Corea mélange, Cuba. American Journal of Science 310, 889–915.
Blanco-Quintero, I.F., Gerya, T.V., Garcia-Casco, A., Castro, A., 2011a. Subduction of young oceanic plates: a numerical study with application to aborted thermal-chemical plumes. Geochemistry, Geophysics, Geosystems 12 (10).
Blanco-Quintero, I.F., Proenza, J.A., Garcia-Casco, A., Tauler, E., Galí, S., 2011b. Serpentinites and serpentinites within a fossil subduction channel: La Corea mélange, eastern Cuba. Geologica Acta 9 (3–4), 389–405.
Blanco-Quintero, I.F., Rojas-Agramonte, Y., Garcia-Casco, A., Kröner, A., Mertz, D.F., Lázaro, C., Blanco-Moreno, J., Renne, P.R., 2011c. Timing of subduction and exhumation in a subduction channel: evidence from slab melts from La Corea mélange (eastern Cuba). Lithos 127, 86–100.
Boschman, L.M., van Hinsbergen, D.J.J., Torsvik, T.H., Spakman, W., Pindell, J.L., 2014. Kinematic reconstruction of the Caribbean region since the Early Jurassic. Earth Science Reviews 138, 102–136.
Cardona, A., Valencia, V., Garzón, A., Montes, C., Ojeda, G., Ruiz, J., Weber, M., 2010. Permian to Triassic I to S-type magmatic switch in the northeast Sierra Nevada de Santa Marta and adjacent regions, Colombian Caribbean: tectonic setting and implications within Pangea paleogeography. Journal of South American Earth Sciences 29, 772–783.
Castro, A., Gerya, T., Garcia-Casco, A., Fernández, C., Díaz-Alvarado, J., Moreno-Ventas, I., Löw, I., 2010. Melting relations of MORB–sediment mélanges in underplated mantle wedge plumes; Implications for the origin of cordilleran-type batholiths. Journal of Petrology 51, 1267–1295.
Centeno-García, E., 2017. Mesozoic tectono-magmatic evolution of Mexico: an overview. Ore Geology Reviews 81, 1035–1052.
Cobiella-Reguera, J.L., 2005. Emplacement of Cuban ophiolites. Geologica Acta 3, 273–294.

Cochrane, R., Spikings, R., Gerdes, A., Ulianov, A., Mora, A., Villagómez, D., Putlitz, B., Chiaradia, M., 2014. Permo–Triassic anatexis, continental rifting and the disassembly of western Pangaea. Lithos 190–191, 383–402.
Gao, S., Rudnick, R.L., Yuan, H.-L., Liu, X.-M., Liu, Y.-S., Xu, W.-L., Ling, W.-L., Ayers, J., Wang, X.-C., Wang, Q.-H., 2004. Recycling lower continental crust in the North China craton. Nature 432, 892–897.
Garcia-Casco, A., Iturralde-Vinent, M.A., Pindell, J., 2008a. Latest Cretaceous collision/accretion between the Caribbean Plate and Caribeana: origin of metamorphic terranes in the Greater Antilles. International Geology Reviews 50, 781–809.
Garcia-Casco, A., Lázaro, C., Torres-Roldán, R.L., Núñez Cambra, K., Rojas Agramonte, Y., Kröner, A., Neubauer, F., Millán, G., Blanco-Quintero, I., 2008b. Partial melting and counterclockwise P-T path of subducted oceanic crust (Sierra del Convento mélange, Cuba). Journal of Petrology 49, 129–161.
Garcia-Casco, A., Torres-Roldán, R.L., Iturralde-Vinent, M.A., Millán, G., Núñez Cambra, K., Lázaro, C., Rodríguez Vega, A., 2006. High pressure metamorphism of ophiolites in Cuba. Geologica Acta 4, 63–88.
Gervilla, F., Proenza, J.A., Frei, R., González-Jiménez, J.M., Garrido, C.J., Melgarejo, J.C., Meibom, A., Díaz-Martinez, R., Lavaut, W., 2005. Distribution of platinum-group elements and Os isotopes in chromite ores from Mayarí-Baracoa Ophiolitic Belt (eastern Cuba). Contributions to Mineralogy and Petrology 150, 589–607.
Gerya, T.V., Yuen, D.A., 2003. Rayleigh–Taylor instabilities from hydration and melting propel 'cold plumes' at subduction zones. Earth and Planetary Science Letters 212, 47–62.
González-Jiménez, J.M., Camprubì, A., Colá, V., Griffin, W.L., Proenza, J.A., O'Reilly, S.Y., Centeno-García, E., Garcia-Casco, A., Belousova, E., Talavera, C., Farré-de Pablo, J., Satsukawa, T., 2017a. The recycling of chromitites in ophiolites from southwestern North America. Lithos 294–295, 53–72.
González-Jiménez, J.M., Gervilla, F., Griffin, W.L., Proenza, J.A., Augé, T., O'Reilly, S.Y., Pearson, N.J., 2012. Os-isotope variability within sulfides from podiform chromitites. Chemical Geology 291, 224–235.
González-Jiménez, J.M., Locmelis, M., Belousova, E., Griffin, William L., Gervilla, F., Kerestedjian, T., O'Reilly, S.Y., Sergeeva, I., Pearson, N.J., 2015. Genesis and tectonic implications of podiform chromitites in the metamorphosed Ultramafic Massif of Dobromirtsi (Bulgaria). Gondwana Research 27, 555–574.
González-Jiménez, J.M., Marchesi, C., Griffin, W.L., Gervilla, F., Belousova, E.A., Garrido, C.J., Romero, R., Talavera, C., Leisen, M., O'Reilly, S.Y., Barra, F., Martin, L., 2017b. Zircon recycling and crystallization during formation of chromite- and Ni-arsenide ores in the subcontinental lithospheric mantle (Serranía de Ronda, Spain). Ore Geology Reviews. https://doi.org/10.1016/j.oregeorev.2017.02.012.
González-Jiménez, J.M., Proenza, J.A., Gervilla, F., Melgarejo, J.C., Blanco-Moreno, J.A., Ruiz-Sánchez, R., Griffin, W.L., 2011. High-Cr and high-Al chromitites from the Sagua de Tánamo district, Mayarí-Cristal Ophiolitic Massif (eastern Cuba): constraints on their origin from mineralogy and geochemistry of chromian spinel and platinum group elements. Lithos 125, 101–121.
Gorczyk, W., Gerya, T.V., Connolly, J.A.D., Yuen, D.A., 2007. Growth and mixing dynamics of mantle wedge plumes. Geology 35, 587–590.
Griffin, W.L., O'Reilly, S.Y., Afonso, J.C., Begg, G.C., 2009. The composition and evolution of lithospheric mantle: a re-evaluation and its tectonic implications. Journal of Petrology 50, 1185–1204.
Griffin, W.L., Afonso, J.C., Belousova, E.A., Gain, S.E., Gong, X.H., González-Jiménez, J.M., Howell, D., Huang, J.X., McGowan, N., Pearson, N.J., Satsukawa, T., Shi, R., Williams, P., Xiong, Q., Yang, J.S., Zhang, M., O'Reilly, S.Y., 2016. Mantle recycling: transition zone metamorphism of Tibetan ophiolitic peridotites and its tectonic implications. Journal of Petrology 57, 655–684.
Iturralde-Vinent, M., 1996. Introduction to Cuban geology and geophysics. Ofiolitas y Arcos Volcánicos de Cuba. Miami, Florida, International Geological Correlation Programme, Project 364, 3–35.
Iturralde-Vinent, M.A., Díaz-Otero, C., Rodríguez-Vega, A., Díaz-Martínez, R., 2006. Tectonic implications of paleontologic dating of Cretaceous–Danian sections of Eastern Cuba. Geologica Acta 4, 89–102.
Iturralde-Vinent, M.A., Garcia-Casco, A., Rojas-Agramonte, Y., Proenza, J.A., Murphy, J.B., Stern, R.G., 2016. The geology of Cuba: a brief overview and synthesis. GSA Today 26 (10), 4–10.
Kamenov, G.D., Perfit, M.R., Lewis, J.F., Goss, A.R., Arévalo Jr., R., Shuster, R.D., 2011. Ancient lithospheric source for Quaternary lavas in Hispaniola. Nature Geoscience 4, 554–557.
Kelemen, P.B., Koga, K., Shimizu, N., 1997. Geochemistry of gabbro sillsin the crust-mantle transition zone of the Oman ophiolite: implications for the origin of the oceanic lower crust. Earth and Planetary Science Letters 146, 475–488.
Kemp, A., Hawkesworth, C., Foster, G., Paterson, B., Woodhead, J., Hergt, J., Gray, C., Whitehouse, M., 2007. Magmatic and crustal differentiation history of granitic rocks from Hf–O isotopes in zircon. Science 315, 980–983.
Keppie, J.D., Nance, R.D., Dostal, J., Ortega-Rivera, A., Miller, B.V., Fox, D., Powell, J.T., Mumma, S.A., Lee, J.K.W., 2004. Mid-Jurassic tectonothermal event superposed on a Paleozoic geological record in the Acatlán Complex of southern Mexico: hotspot activity during the breakup of Pangea. Gondwana Research 7, 239–260.
Kirsch, M., Keppie, J.D., Murphy, J.B., Lee, J.K.W., 2013. Arc plutonism in a transtensional regime: the late Paleozoic Totoltepec pluton, Acatlán Complex, southern Mexico. International Geology Review 55, 263–286.
Kirsch, M., Keppie, D.J., Murphy, B., Solari, L., 2012. Permian–Carboniferous arc magmatism and basin evolution along the western margin of Pangea: geochemical and geochronological evidence from the eastern Acatlán Complex, southern Mexico. Geological Society of America Bulletin 124, 1607–1628.
Lázaro, C., Blanco-Quintero, I.F., Proenza, J.A., Rojas-Agramonte, Y., Neubauer, F., Núñez-Cambra, K., Garcia-Casco, A., 2016. Petrogenesis and $^{40}Ar/^{39}Ar$ dating of proto-forearc crust in the Early Cretaceous Caribbean arc: the La Tinta mélange (eastern Cuba) and its easterly correlation in Hispaniola. International Geology Review 58 (4), 1020–1040.
Lázaro, C., Garcia-Casco, A., Blanco-Quintero, I.F., Rojas- Agramonte, Y., Corsini, M., Proenza, J.A., 2015. Did the Turonian–Coniacian plume pulse trigger subduction initiation in the Northern Caribbean? Constraints from $^{40}Ar/^{39}Ar$ dating of the Moa-Baracoa metamorphic sole (eastern Cuba). International Geology Review 57 (5–8), 919–942.
Lázaro, C., Garcia-Casco, A., Rojas-Agramonte, Y., Kröner, A., Neubauer, F., Iturralde-Vinent, M., 2009. Fifty-five-million-year history of oceanic subduction and exhumation at the northern edge of the Caribbean plate (Sierra del Convento mélange, Cuba). Journal of Metamorphic Geology 27, 19–40.
Leal-Mejía, H., Shaw, R., Melgarejo, J.C., 2011. Phanerozoic granitoid magmatism in Colombia and the tectonic-magmatic evolution of the Colombian Andes. In: Cediel, F. (Ed.), Petroleoum Geology of Colombia – Regional Geology of Colombia. Fondo Editorial. Universidad EAFIT, Medellín, 225pp.
Lewis, J.F., Draper, G., Proenza, J.A., Espaillat, J., Jiménez, J., 2006. Ophiolite-related ultramafic rocks (serpentinites) in the Caribbean region: a review of their occurrence, composition, origin, emplacement and nickel laterite soils. Geologica Acta 4, 237–263.
Lian, D., Yang, J., Dilek, Y., Wu, W., Zhang, Z., Xiong, F., Liu, F., Zhou, W., 2017. Diamond, Moissanite and other unusual minerals in podiform chromitites from the Pozanti-Karsanti ophiolite, southern Turkey: implications for the deep mantle origin and ultra-reducing conditions in podiform chromitite. American Mineralogist. https://doi.org/10.2138/am-2017-5850.
Lönngren, M., Kojonen, K., 2005. Dissolution of chromitite ore for platinum group elements and gold analysis, Ray–Iz ophiolitic complex, Polar Urals. In: Törmänen, T.O., Alapieti, T.T. (Eds.), 10th International Platinum Symposium: 'Platinum-group Elements — from Genesis to Beneficiation and Environmental Impact', August 8–11, 2005, Oulu, Finland (Extended Abstracts).
Marchesi, C., Garrido, C.J., Bosch, D., Proenza, J.A., Gervilla, F., Monié, P., Rodriguez-Vega, A., 2007. Geochemistry of Cretaceous magmatism in eastern Cuba: recycling of North American continental sediments and implications for subduction polarity in the Greater Antilles Paleo-arc. Journal of Petrology 48, 1813–1840.
Marchesi, C., Garrido, C.J., Godard, M., Proenza, J.A., Gervilla, F., Blanco-Moreno, J., 2006. Petrogenesis of highly depleted peridotites and gabbroic rocks from the Mayarí-Baracoa Ophiolitic Belt (eastern Cuba). Contributions to Mineralogy and Petrology 151, 717–736.
Marchesi, C., González-Jiménez, J.M., Gervilla, F., Garrido, C.J., Griffin, W.L., O'Reilly, S.Y., Proenza, J.A., Pearson, N.J., 2011. In situ Re–Os isotopic analysis of platinum-group minerals from the Mayarí–Cristal ophiolitic massif (Mayarí–Baracoa Ophiolitic Belt, eastern Cuba): implications for the origin of Os-isotope heterogeneities in podiform chromitites. Contributions to Mineralogy and Petrology 161, 977–990.
Marschall, H.R., Schumacher, J.C., 2012. Arc magmas sourced from mélange diapirs in subduction zones. Nature Geoscience 5, 862–867.
McGowan, N.M., Griffin, W.L., González-Jiménez, J.M., Belousova, E.A., Afonso, J., Shi, R., McCammon, C.A., Pearson, N.J., O'Reilly, S.Y., 2015. Tibetan chromitites: excavating the slab graveyard. Geology 43, 179–182.
Nance, R.D., Miller, B.V., Keppie, J.D., Murphy, J.B., Dostal, J., 2006. Acatlán Complex, southern Mexico: record spanning the assembly and breakup of Pangea. Geology 34, 857–860.
O'Reilly, S.Y., Zhang, M., Griffin, W.L., Begg, G., Hronsky, J., 2009. Ultradeep continental roots and their oceanic remnants: a solution to the geochemical "mantle reservoir" problem? Lithos 112, 1043–1054.
Ortega-Obregón, C., Solari, L., Gómez-Tuena, A., Elías-Herrera, M., Ortega-Gutiérrez, F., Macías-Romo, C., 2014. Permian–Carboniferous arc magmatism in southern Mexico: U–Pb dating, trace element and Hf isotopic evidence on zircon grains of earliest subduction beneath the western margin of Gondwana. International Journal of Earth Sciences (Geologische Rundschau) 103, 1287–1300.
Peltonen, P., Manttani, I., Huhma, H., Kontinen, A., 2003. Archean zircon grains from the mantle: the Jormua ophiolite revisited. Geology 31, 645–648.
Pindell, J., Kennan, L., 2009. Tectonic evolution of the Gulf of Mexico, Caribbean and northern South America in the mantle reference frame. An update. In: James, K.H., Lorente, M.A., Pindell, J.L. (Eds.), The Origin and Evolution of the Caribbean Plate, London Geological Society Special Publications, 328, pp. 1–55.
Pindell, J.L., Maresch, W.V., Martens, U., Stanek, K.P., 2012. The greater antillean arc: early Cretaceous origin and proposed relationship to Central American subduction mélanges: implications for models of Caribbean evolution. International Geology Review 54, 131–143.
Proenza, J.A., Díaz-Martínez, R., Iriondo, A., Marchesi, C., Melgarejo, J.C., Gervilla, F., Garrido, C.J., Rodríguez-Vega, A., Lozano-Santacruz, R., Blanco-Moreno, J.A., 2006. Primitive island-arc Cretaceous volcanic rocks in eastern Cuba: the Téneme Formation. Geologica Acta 4, 103–121.
Proenza, J.A., Gervilla, F., Melgarejo, J.C., Bodinier, J.L., 1999. Al- and Cr-rich chromitites from the Mayarí-Baracoa ophiolitic belt (eastern Cuba); consequence of interaction between volatile-rich melts and peridotites in suprasubduction mantle. Economic Geology 94, 547–566.

Proenza, J.A., Gervilla, F., Melgarejo, J.C., Revé, D., Rodríguez, G., 1998. Las cromititas ofiolíticas del yacimiento Mercedita (Cuba). Un ejemplo de cromitas ricas en Al en la zona de transición manto-corteza. Acta Geologica Hispanica 33, 179–212.

Proenza, J.A., Gervilla, F., Melgarejo, J.C., Vera, O., Alfonso, P., Fallick, A., 2001a. Genesis of sulfide-rich chromite ores by the interaction between chromitite and pegmatitic olivine-norite dikes in the Potosí Mine (Moa-Baracoa ophiolitic massif, eastern Cuba). Mineralium Deposita 36, 658–669.

Proenza, J.A., Melgarejo, J.C., Gervilla, F., Llovet, X., 2001b. Y-zirconolita en cromititas ofioliticas de Cuba oriental. Implicaciones petrogeneticas. Boletín de la Sociedad Española de Mineralogía 24A, 39–40 (abstr.).

Pushcharovsky, Y. (Ed.), 1988. Mapa geoloìgico de la Repuìblica de Cuba escala 1:250 000: Academias de Ciencias de Cuba y la URSS.

Robinson, P.T., Bai, W.-J., Malpas, J., Yang, J.-S., Zhou, M.-F., Fang, Q.-S., Hu, X.-F., Cameron, S., Staudigel, H., 2004. Ultra-high pressure minerals in the Luobusa ophiolite, Tibet, and their tectonic implications. Geological Society London Special Publication 226, 247–271.

Robinson, P.T., Trumbull, R.B., Schmitt, A., Yang, J.S., Li, J.W., Zhou, M.F., Erzinger, J., Dare, S., Xiong, F., 2015. The origin and significance of crustal minerals in ophiolitic chromitites and peridotites. Gondwana Research 27, 486–506.

Rojas-Agramonte, Y., Kröner, A., Garcia-Casco, A., Kemp, T., Hegner, E., Pérez, M., Barth, M., Liu, D., Fonseca-Montero, A., 2010. Zircon ages, Sr–Nd–Hf isotopic compositions, and geochemistry of granitoids associated with the northern ophiolite mélange of Central Cuba: tectonic implication for Late Cretaceous magmatism in the Northwestern Caribbean. American Journal of Science 310, 1453–1479.

Rojas-Agramonte, Y., Kröner, A., Garcia-Casco, A., Somin, M., Iturralde-Vinent, M., Mattinson, J., Trujillo, G.M., Sukar, K., Rodríguez, M.P., Carrasquilla, S., Wingate, M.T.D., Liu, D.Y., 2011. Timing and evolution of Cretaceous island arc magmatism in central Cuba: implications for the history of arc systems in the northwestern Caribbean. The Journal of Geology 119, 619–640.

Rojas-Agramonte, Y., Garcia-Casco, A., Kemp, A., Kröner, A., Proenza, J.A., Lázaro, C., Liu, D., 2016. Recycling and transport of continental material through the mantle wedge above subduction zones: a Caribbean example. Earth and Planetary Science Letters 436, 93–107.

Savelieva, G.N., Suslov, P.V., Larionov, A.N., 2007. Vendian tectono-magmatic events in mantle ophiolitic complexes of the Polar Urals: U–Pb dating of zircon from chromitite. Geotectonics 41, 105–113.

Savelieva, G.N., Suslov, P.V., Larionov, A.N., Berezhnaya, N.G., 2006. Age of zircon grains from chromitites in the residual ophiolitic rocks as a reflection of upper mantle magmatic events. Doklady Earth Sciences 411A (9), 1401–1406.

Scholl, D.W., von Huene, R., 2009. Implications of estimated magmatic additions and recycling losses at the subduction zones of accretionary (non-collisional) and collisional (suturing) orogens. Geological Society, London, Special Publications 318, 105–125.

Shi, R., Alard, O., Zhi, X., O'Reilly, S.Y., Pearson, N.J., Griffin, W.L., Zhang, M., Chen, X., 2007. Multiple events in the Neo-Tethyan oceanic upper mantle:evidence from Ru–Os–Ir alloys in the Luobusa and Dongqiao ophiolitic podiform chromitites, Tibet. Earth and Planetary Science Letters 261, 33–48.

Solari, L.A., Ortega-Gutiérrez, F., Elías-Herrera, M., Ortega-Obregón, C., Macías-Romo, C., Reyes-Salas, M., 2014. Detrital provenance of the Grenvillian Oaxacan Complex, southern Mexico: a zircon perspective. International Journal of Earth Sciences 103, 1301–1315.

Spandler, C., Pirard, C., 2013. Element recycling from subducting slabs to arc crust: a review. Lithos 170–171, 208–223.

Stern, R.J., 2002. Subduction zones. Reviews of Geophysics 40 (4), 3–38.

Stern, R.J., Ali, K.A., Liegois, J.P., Johnson, P.R., Kozdrojs, W., Kattan, F.H., 2010. Distribution and significance of pre-Neoproterozoic zircon grains in juvenile Neoproterozoic igneous rocks of the Arabian–Nubian shield. American Journal of Science 310, 791–811.

Talavera-Mendoza, O., Ruiz, J., Gehrels, G.E., Meza-Figueroa, D., Vega-Granillo, R., Campa-Uranga, M.F., 2005. U-Pb geochronology of the Acatlán Complex and implications for the Paleozoic paleogeography and tectonic evolution of southern Mexico. Earth and Planetary Science Letters 235, 682–699.

Tang, Y.-J., Zhang, H.-F., Ying, J.-F., Su, B.-X., 2013. Widespread refertilization of cratonic and circum-cratonic lithospheric mantle. Earth Science Reviews 118, 45–68.

Torró, L., Garcia-Casco, A., Proenza, J.A., Blanco-Quintero, I.F., Gutiérrez-Alonso, G., Lewis, J.F., 2016. High-pressure greenschist to blueschist facies transition in the Maimón Formation (Dominican Republic) suggests mid-cretaceous subduction of the Early Cretaceous Caribbean arc. Lithos 266–267, 309–331.

Torró, L., Proenza, J.A., Marchesi, C., Garcia-Casco, A., Lewis, J.F., 2017. Petrogenesis of meta-volcanic rocks from the Maimón formation (the Dominican Republic): geochemical record of the nascent Greater Antilles paleo-arc. Lithos 278–281, 255–273.

Torró, L., Proenza, J.A., Rojas-Agramonte, Y., Garcia-Casco, A., Yang, J.H., Yang, Y.H., 2018. Recycling in the subduction factory: Archaean to Permian zircons in the oceanic Cretaceous Caribbean island-arc (Hispaniola). Gondwana Research 54, 23–37.

Weber, B., Schulze, C.H., 2014. Early Mesoproterozoic (>1.4 Ga) ages from granulite basement inliers of SE Mexico and their implications on the Oaxaquia concept – evidence from U–Pb and Lu–Hf isotopes on zircon. Revista Mexicana de Ciencias Geológicas 31, 377–394.

Xiong, F., Yang, J., Robinson, P.T., Xu, X., Liu, Z., Li, Y., Li, J., Chen, S., 2015. Origin of podiform chromitite, a new model based on the Luobusa ophiolite, Tibet. Gondwana Research 27, 525–542.

Xu, X., Yang, J., Robinson, P., Xiong, F., Ba, D., Guo, G., 2015. Origin of ultrahigh pressure and highly reduced minerals in podiform chromitites and associated peridotites of the Luobusa ophiolite, Tibet. Gondwana Research 27, 686–700.

Yamamoto, S., Komiya, T., Yamamoto, H., Kaneko, Y., Terabayashi, M., Katayama, I., Iizuka, T., Maruyama, S., Yang, J., Kon, Y., Hirata, T., 2013. Recycled crustal zircon grains from podiform chromitites in the Luobusa ophiolite, southern Tibet. The Island Arc 22, 89–103.

Yang, J.S., Robinson, P.T., Dilek, Y., 2014. Diamonds in ophiolites. Elements 10, 127–130.

Yang, J.S., Meng, F., Xu, S., Robinson, P.T., Dilek, Y., Makeyev, A.B., Wirth, R., Wiedenbeck, M., Cliff, J., 2015. Diamonds, native elements and metal alloys from chromitite of the Ray-Iz ophiolite of the Polar Urals. Gondwana Research 27, 459–485.

Zhou, M.F., Robinson, P.T., Su, B.-X., Gao, J.-F., Li, J.-W., Yang, J.-S., Malpas, J., 2014. Compositions of chromite, associated minerals, and parental magmas of podiform chromite deposits. The role of slab contamination of asthenospheric melts in suprasubduction zone environments. Gondwana Research 26, 262–283.